



Quantification of amyloid PET for future clinical use: a state-of-the-art review

Hugh G. Pemberton^{1,2,3} · Lyduine E. Collij⁴ · Fiona Heeman⁴ · Ariane Bollack² · Mahnaz Shekari^{5,6,7} · Gemma Salvadó^{5,8} · Isadora Lopes Alves^{4,9} · David Vallez Garcia⁴ · Mark Battle^{1,8} · Christopher Buckley¹ · Andrew W. Stephens¹⁰ · Santiago Bullich¹⁰ · Valentina Garibotto^{11,12} · Frederik Barkhof^{2,3,4} · Juan Domingo Gispert^{5,6,7,13} · Gill Farrar¹ · on behalf of the AMYPAD consortium

Received: 6 December 2021 / Accepted: 25 March 2022 / Published online: 7 April 2022
© The Author(s) 2022

Abstract

Amyloid- β (A β) pathology is one of the earliest detectable brain changes in Alzheimer's disease (AD) pathogenesis. The overall load and spatial distribution of brain A β can be determined in vivo using positron emission tomography (PET), for which three fluorine-18 labelled radiotracers have been approved for clinical use. In clinical practice, trained readers will categorise scans as either A β positive or negative, based on visual inspection. Diagnostic decisions are often based on these reads and patient selection for clinical trials is increasingly guided by amyloid status. However, tracer deposition in the grey matter as a function of amyloid load is an inherently continuous process, which is not sufficiently appreciated through binary cut-offs alone. State-of-the-art methods for amyloid PET quantification can generate tracer-independent measures of A β burden. Recent research has shown the ability of these quantitative measures to highlight pathological changes at the earliest stages of the AD *continuum* and generate more sensitive thresholds, as well as improving diagnostic confidence around established binary cut-offs. With the recent FDA approval of aducanumab and more candidate drugs on the horizon, early identification of amyloid burden using quantitative measures is critical for enrolling appropriate subjects to help establish the optimal window for therapeutic intervention and secondary prevention. In addition, quantitative amyloid measurements are used for treatment response monitoring in clinical trials. In clinical settings, large multi-centre studies have shown that amyloid PET results change both diagnosis and patient management and that quantification can accurately predict rates of cognitive decline. Whether these changes in management reflect an improvement in clinical outcomes is yet to be determined and further validation work is required to establish the utility of quantification for supporting treatment endpoint decisions. In this state-of-the-art review, several tools and measures available for amyloid PET quantification are summarised and discussed. Use of these methods is growing both clinically and in the research domain. Concurrently, there is a duty of care to the wider dementia community to increase visibility and understanding of these methods.

Keywords Brain · Amyloid · PET · Quantification · Alzheimer's · Dementia · Centiloid · SUVr

Abbreviations

AD	Alzheimer's disease	CL	Centiloid
ADNI	Alzheimer's Disease Neuroimaging Initiative	CBF	Cerebral blood flow
A β	Amyloid- β	CSF	Cerebrospinal fluid
A/T/N	Amyloid/tau/neurodegeneration	FDA	Food and Drug Administration
AIBL	Australian Imaging, Biomarkers and Lifestyle	EMA	European Medicines Authority
		GAAIN	Global Alzheimer's Association Interactive Network
		MCI	Mild cognitive impairment
		PET	Positron emission tomography
		PCA	Principal component analysis
		PNHS	Prognostic and natural history study
		SUVr	Standardised uptake value ratio

This article is part of the Topical Collection on Neurology – Dementia

✉ Hugh G. Pemberton
hugh.pemberton@ge.com

Extended author information available on the last page of the article

SPM Statistical parametric mapping
 SCD Subjective cognitive decline

Introduction

Amyloid- β and the AD continuum

Alzheimer's disease (AD) is the most common cause of dementia, accounting for 60–80% of cases above 65 years of age [1]. One of the earliest detectable brain changes in AD pathogenesis is amyloid- β (A β) plaque accumulation [2–4]. However, historically, AD has been diagnosed solely based on symptomatology, with a definite diagnosis only possible by *post-mortem* examination. With the recent arrival and increased availability of biomarkers for AD pathology, there has been a shift towards biomarker-based diagnosis, which can be appreciated in the 2007 research diagnosis criteria from the International Working Group [5, 6]. Updated in 2021 [7], the guidelines now further highlight amyloid's central role in the AD diagnostic process. In research settings, a biomarker-only classification scheme has even been proposed, the amyloid/tau/neurodegeneration (A/T/N) framework [8], which further highlights the shift towards a biological definition of the disease independent of clinically defined diagnostic schemes. Detection of abnormal A β only, referred to as “Alzheimer's pathologic change” (A+/T–), is considered the essential first step and if followed by a pathological change in tau progresses to the classification of AD (A+/T+) — with or without dementia. Amyloid biomarkers have been used as part of the A/T/N framework in large validation studies of population-based cohorts [9, 10], memory clinic populations [11, 12], cognitively unimpaired subjects [13], and longitudinal cognitive outcomes [9, 11, 13]. The central role of amyloid pathology across the AD *continuum* has been of major interest for both AD clinical research and drug development [14–17]. Alongside the development of cerebrospinal fluid (CSF) and blood-based biomarkers, molecular imaging using positron emission tomography (PET) plays an increasingly important role in determining biomarker status [18].

Amyloid PET

The use of amyloid PET allows for the *in vivo* visualisation and quantification of A β protein fibrillary deposits, directly providing information on the total load and spatial distribution of A β pathology. Three fluorine-18 amyloid PET tracers are currently available for routine clinical use (Fig. 1) and have been validated against Consortium to Establish a Registry for Alzheimer's Disease (CERAD) pathology as the gold standard. These radiotracers are [¹⁸F]florbetapir (Amyvid™; Avid Radiopharmaceuticals; approved in

2012) [19], [¹⁸F]flutemetamol (Vizamyl™; GE Healthcare; approved in 2013) [20], and [¹⁸F]florbetaben (Neuraceq™; Life Molecular Imaging; approved in 2014) [21]. Each of these radiotracers has different pharmacokinetics, chemical structure, and binding site/properties. However, they have all been approved by the Food and Drug Administration (FDA) and European Medicines Authority (EMA) for routine clinical use, and have local regulatory approval in other countries, such as Japan and Korea. The tracers are also widely used by the research community. In addition, other known compounds such as the carbon-11 labelled Pittsburgh compound B ([¹¹C]PiB) [22] and [¹⁸F]NAV4694 [18, 23] are available for investigational use only.

Clinical utility of amyloid PET

Routine clinical use of amyloid PET tracers involves visual assessment and binary categorisation of scans, based on tracer-specific manufacturers' guidelines [24–26]. Classification is either *negative* (predominantly white matter uptake) or *positive* (binding in one or more cortical brain regions, or the striatum for [¹⁸F]flutemetamol and [¹¹C]PiB). Certified readers are required by the regulatory authorities to complete and pass a training program specific to each radiotracer [27–29]. The visual assessment scales and guidelines are different for each radiotracer. However, high inter-rater agreement for visual rating protocols has been demonstrated for all ¹⁸F-labelled amyloid tracers [30], suggesting that visual interpretation of amyloid imaging by experts is not dependent on the rating protocol. Furthermore, efforts to create a universal visual assessment protocol for all amyloid imaging tracers are underway [31].

Over the past decade, many studies have demonstrated the level of analytical and clinical validity of amyloid PET in routine clinical practice [25, 29, 32–40]. More specifically, real-world studies have shown that disclosure of amyloid PET imaging results leads to a change in etiological diagnosis in approximately 25–31% of cases [33, 35, 36], significant increases in diagnostic confidence [33, 36, 38–40], and changes in patient management in approximately 37–72% of cases [35–38]. Appropriate use criteria have also been published for amyloid PET [41]. However, recent evidence suggests that patients beyond the appropriate use criteria can also benefit from amyloid PET through changes in management and diagnosis [42]. For example, research has suggested that anti-amyloid strategies could be a relevant approach to slow disease progression in Parkinson's disease and Lewy body dementia [43, 44]. Also, in subjective cognitive decline (SCD) patients, for whom a positive or negative amyloid status can increase diagnostic confidence [33, 34, 37]. The largest clinical utility study to date is the Imaging Dementia-Evidence for Amyloid Scanning (IDEAS) study, which was designed to investigate

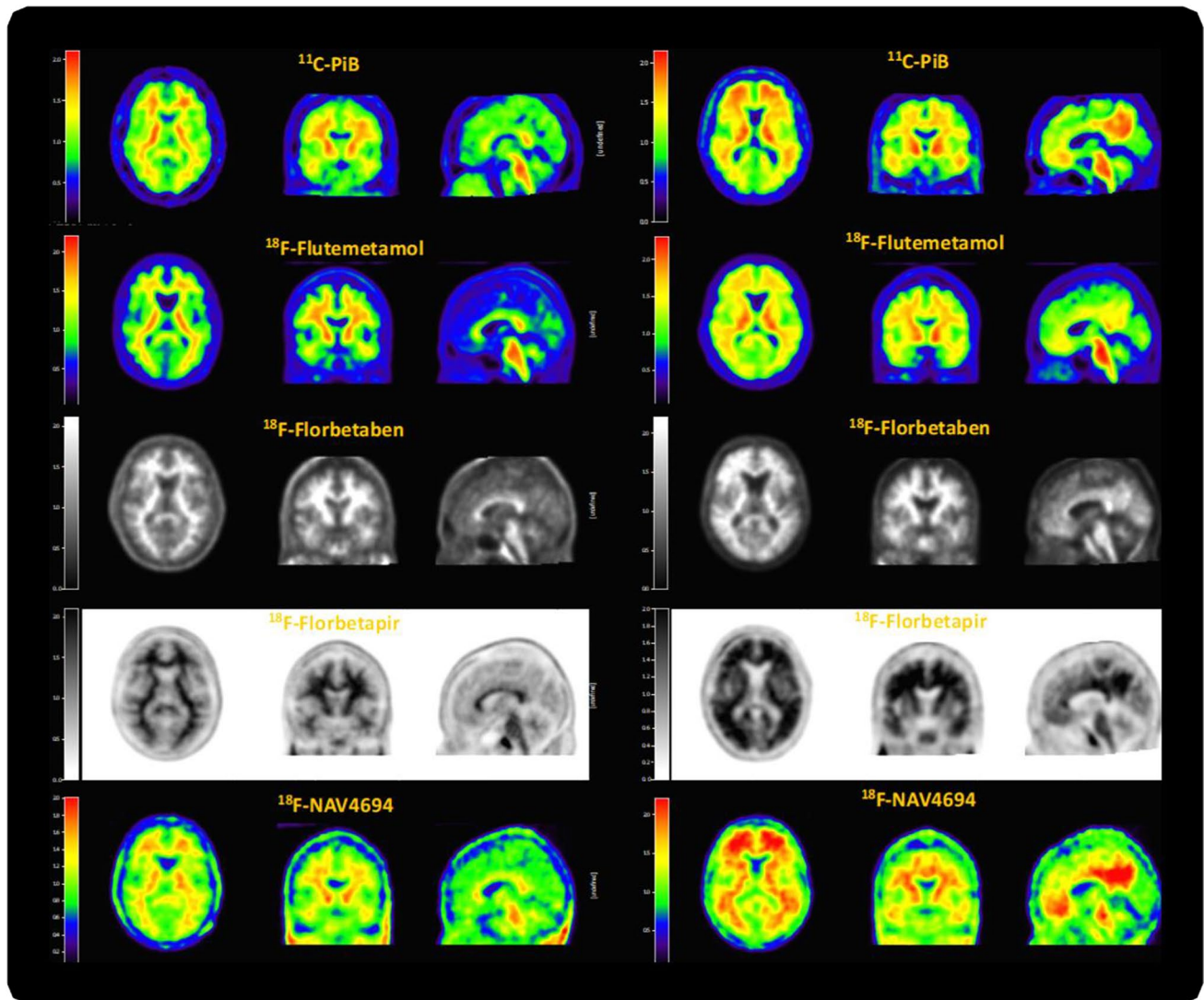


Fig. 1 Illustrative PET images derived from the five most commonly used amyloid tracers on different patients. The left column shows AB negative subjects (all ~0 Centiloid) and right column shows AB positive subjects (all ~50 Centiloid, for further details, see “Centiloid scaling” section). Colour schemes used for regulatory approved tracers are in line with each of their FDA label prescribing information:

[^{18}F]flutemetamol (https://www.accessdata.fda.gov/drugsatfda_docs/label/2016/203137s0051bl.pdf), [^{18}F]florbetaben (https://www.accessdata.fda.gov/drugsatfda_docs/label/2014/204677s0001bl.pdf), [^{18}F]florbetapir (https://www.accessdata.fda.gov/drugsatfda_docs/label/2012/202008s0001bl.pdf)

the clinical utility of amyloid PET. The study enrolled over 18,000 patients from 946 dementia specialists at 595 centres in America [34]. Of the 11,409 patients completing study procedures, the composite endpoint changed in 4159 of 6905 patients with MCI (60.2%), the etiological diagnosis changed from AD to non-AD in 2860 (25.1%), and from non-AD to AD in 1201 (10.5%) cases, which was linked with changes in clinical management within 90 days. Whether these changes in management reflect an improvement in clinical outcomes for dementia patients is yet to be determined.

Global multi-centre studies adopting amyloid PET

Global multi-centre studies and consortia aiming to unravel the influence, prognostic value, and role of amyloid deposition in the AD timeline have been ongoing for some time. The Alzheimer’s Disease Neuroimaging Initiative (ADNI) study began in 2005 [45] and has acquired amyloid PET in thousands of mainly MCI patients [46–48] (<http://adni.loni.usc.edu/>). The first results from the Australian Imaging, Biomarkers and Lifestyle (AIBL) study were published in 2009 [49] and has continued to monitor over 1,000 volunteers

(<http://adni.loni.usc.edu/category/aibl-study-data/>). More recently, in 2016, the AMYPAD consortium was initiated involving multiple academic and private research partners (<https://amypad.eu/>). AMYPAD consists of two substudies: (i) the diagnostic and patient management study (DPMS) [50], assessing amyloid PET's impact on clinical management and diagnosis where quantitative measures will be the secondary endpoint; and (ii) the prognostic and natural history study (PNHS) [51]. In the PNHS, quantitative measures are the primary endpoint and amyloid PET is used to understand the development of AD in the pre-dementia phase of the disease, including cognitively unimpaired, SCD, and MCI participants. Given these goals, another major objective of AMYPAD is the development and validation of robust standardised methodology for quantitatively measuring brain amyloid [52], see “Future directions” section later in this review for an overview of AMYPAD's ongoing studies. Studies such as these highlight the importance of amyloid PET and quantitative measures across the AD continuum, while visual reading remains the most common method of A β pathology in clinical routine.

Challenges of amyloid PET visual assessment across the clinical spectrum

Phase III autopsy validation studies have shown that binary classification through visual assessment is approximately 90% accurate in advanced clinical and end-of-life subjects, providing a useful stratification of A β status for clinical routine, clinical trials, and research purposes [20, 21, 27]. In a heterogeneous clinical population, visual assessment can be challenged by partial volume effects compounded by cortical thinning or atrophy, which in turn raises the question of whether or not to perform partial volume correction (PVC). The field remains divided on this issue, where recent evidence suggests that PVC can increase sensitivity for detecting early stage cerebral amyloidosis [53], but other studies comparing techniques have proven inconclusive [54, 55]. In addition, comorbidities such as normal pressure hydrocephalus [56] or other neurodegenerative disorders can further complicate visual assessments [29, 57–60]. However, the proportion of pre-dementia patients assessed in memory clinics has significantly increased over the past few years, with up to ~25% of patients presenting with SCD [61]. In these subjects, amyloid deposition may be emerging or focal [62], which makes visual assessment more challenging, especially by less experienced readers [63]. In such cases, the dichotomous approach is more prone to subjectivity, as it heavily relies on the prior experience of the clinician, resulting in higher inter-rater variability [19, 30, 64–66]. Therefore, adjunct quantitative measures of amyloid deposition and more sensitive thresholds are beneficial [25, 67–69]. In addition, quantification could hold a range of benefits

and clinical utility on top of current binary classification, such as improvements in diagnostic confidence, prediction of cognitive decline, and changes to patient management [58, 70–74]. Similar utility has been shown for other neurological disorders, for example, quantification of regional atrophy patterns in dementia [75–78] and traumatic brain injury [79, 80]; hippocampal sclerosis and quantitative T2 signal in temporal lobe epilepsy [81–84]; stroke severity quantification by critical care physicians [85, 86]; pre-surgical planning and survival prediction in glioma resection [87, 88]; and lesion load measurements in multiple sclerosis [89–91]. The various quantitative measures available for amyloid PET quantification are discussed in detail later in the review.

Aims of this state-of-the-art review

In this review, methods for quantification of static amyloid PET scans are summarised and compared along with a discussion of the overall utility of amyloid PET quantification in routine clinical practice, observational research, and clinical trials. The general aim is to facilitate greater understanding and wider use of sensitive standardised methodologies for measuring A β pathology. More specifically, accurate cross-sectional and longitudinal measurement of brain amyloid pathology can support the use of amyloid PET biomarkers in clinical and research settings, by providing information on the extent of pathology. This could include the evaluation of both early and established amyloid pathology, improving our understanding of disease development, and consequently optimise individualised risk stratification. Full quantification using dynamic PET acquisition and determination of the non-displaceable binding potential (BP_{ND}) were beyond the scope of this review; as such, the methods covered in this review constitute semi-quantification of amyloid PET. Indeed, factors such as acquisition time window and regional cerebral blood flow can impact methods based on static acquisitions, although the latter does not play a major role in an early AD population [92, 93]. For a review on the value of full PET quantitation, see Lammertsma [94].

Quantitative measures for clinical assessment of amyloid burden

Quantification of static amyloid PET scans can be performed using software packages to calculate both regional and composite levels of amyloid burden. Importantly, these packages generate a continuous measure of amyloid burden which can be used in addition to dichotomous visual reads. Currently available measures are the more commonly used standardised uptake value ratio (SUVR) [95], the Centiloid (CL) scale [74, 96], and reference-based z-scores [97], while the more recent methods include the A β load [98], A β index

[99], and AMYQ [100]. Both CL and z-scores are calculated based on SUVr, whereas the emerging methods use different approaches to select the target and reference regions for segmenting regions of interest (ROIs). In addition, each method provides a unique unit/scale and specific metric for quantification, which motivated inclusion in this review. A key area of current research focusses on the potential sensitivity of visual assessment and quantification methods to variation in scanners [101], reconstruction algorithms [102–104], scanning time, and scanning window [93, 105, 106], all of which can affect both visual assessment and quantification. See “[Future directions](#)” later in this review for an overview of ongoing technical validation studies. While these quantification measures are becoming increasingly common for research purposes, some of these metrics have also been used in clinical practice and trial settings. Quantification could supplement visual inspection of amyloid PET imaging, especially for (i) less experienced readers [63]; (ii) equivocal (“grey zone”) cases [107, 108] where diagnostic confidence is low [109]; and (iii) for assessing isolated regional uptake [57, 110]. In clinical trials, quantification can be used to better guide patient enrolment and for therapy response monitoring [111–114].

Standardised uptake value ratio

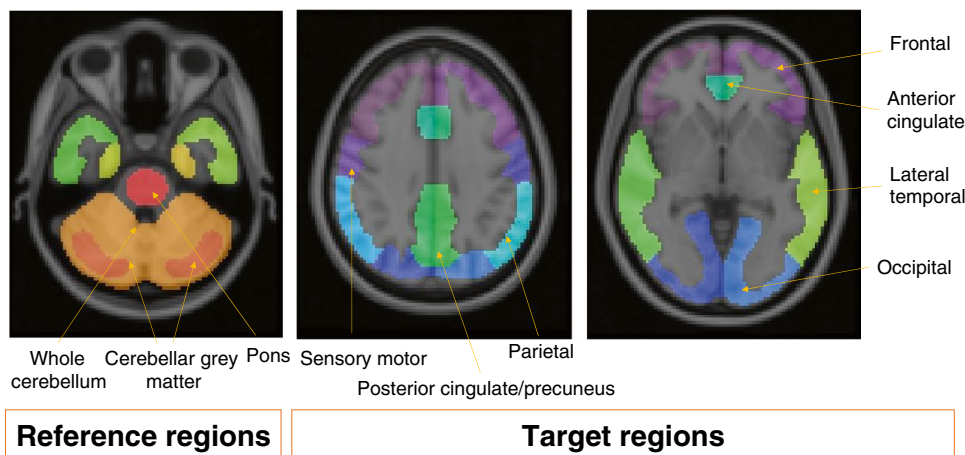
The most widely used measure for quantifying amyloid burden is the SUVr. It is a simplified method based on computing the ratio of tracer uptake between a target region and a reference region in a late (static) PET acquisition, when the radiotracer is expected to have reached pseudo-equilibrium [95] (Fig. 2). Target regions can include either individual regions or be a composite of several (cortical) regions. Common ROIs in the amyloid PET radiotracer product labels include the medial orbital frontal cortex, anterior cingulate, lateral temporal lobes,

precuneus, posterior cingulate, parietal lobe, and striatum. On the other hand, reference regions should ideally have no specific tracer binding, similar tissue characteristics/kinetics as the target regions, and tracer uptake in reference region should be unaffected by the disease under investigation, making the cerebellar cortex a suitable reference regions for amyloid tracers in most cases [94, 115]. Alternative reference regions have been proposed, such as the pons, whole cerebellum, and subcortical white matter, as their use generally results in increased stability of quantification over time [116–118].

Various software packages are clinically available (see “[Regulatory approved tools and research methods for amyloid PET quantification](#)” section below) to quantify brain amyloid using SUVr. Using these software approaches, optimal SUVr cut-offs for amyloid positivity have been defined using various approaches and for different purposes: receiver operating characteristics for differential diagnosis [119], comparison with histological findings [19, 20], and using young healthy adults as a definition for amyloid negativity [120].

SUVr is the most widely used and established metric [121], having been implemented in several recent trials to assess treatment efficacy [122–128]. However, accurate measurement and cut-off values are highly dependent on the chosen tracer, reference region (Fig. 2), and delineation method [74, 129, 130], which challenges the pooling of multi-centre SUVr data across tracers [131]. In addition, there is high variability in longitudinal results [93, 132], which limits the power in detecting genuine biological differences. SUVr values can also vary based on partial volume averaging effects [133, 134]. However, PVC intrinsically amplifies noise in trying to reduce bias and, therefore, a given PVC method needs to be finely tuned to the particular image characteristics so that the beneficial effects of the method outweigh anything detrimental.

Fig. 2 Example of the most common reference and target regions used when generating SUVr



Centiloid scaling

As the use of different amyloid PET tracers grew in both clinical and research settings, there was a need for inter-tracer standardisation of the SUVR metric in multi-centre collaborations. To this end, the CL scale was developed [74], which is an unbounded 0 (mean grey matter signal of young healthy controls) to 100 (typical AD patient signal) scale that conveys a single patient's amyloid burden based on two anchor points using the [¹¹C]PiB SUVR from the Global Alzheimer's Association Interactive Network (GAAIN) reference dataset (<http://www.gaain.org/CL-project>). The main aims of the CL scale were to (i) simplify and expedite direct comparison of Aβ PET results across sites and studies; (ii) outline the earliest thresholds for amyloid positivity and define the range of positivity in AD; (iii) robustly quantify longitudinal change; and (iv) facilitate inter-tracer comparisons [74]. Since then, several studies have tested the scale's validity and used it to improve the harmonisation and standardisation of Aβ PET quantification across tracers, scanners, and analytical implementations [52, 96, 104, 118, 135–144].

The CL approach allows any site using amyloid PET to follow a multi-step process to generate a CL scaling from their own local Aβ PET data. The basic principle is to scale the ¹⁸F-labelled tracers' SUVR to equivalent [¹¹C]PiB SUVR, and this is further transformed to the 0–100 scale mentioned above. This process consists of a validation of the local pipeline using the GAAIN data and then the application to a new tracer [74, 138]. PET processing for CL quantification is often implemented through statistical parametric mapping (SPM) but other methods are available, including those without the use of an accompanying MRI [96, 145]. Routinely, PET images are first co-registered to their corresponding T1-weighted MR images and subsequently transformed to MNI space. Next, PET images are intensity normalised often using the whole cerebellum as the primary reference region, and other reference regions include pons, cerebellar grey matter, and whole cerebellum plus brainstem. Finally, CL values are generated using the mean values of the standard CL target region based on a previously calibrated transformation [74]. The team behind the CL project and producers of the approved fluorine-18 labelled radiotracers have made

progress in deriving and verifying conversion formulae that enable translation of non-[¹¹C]PiB Aβ PET semi-quantitative values to standardised [¹¹C]PiB measures [52, 96, 136, 143], see Table 1 for conversion equations using the standard CL processing pipeline. However, please note that the CL method can be applied to any non-standard pipeline, thus leading to a potentially unlimited number of conversion equations.

Implementation

Since its development in 2015, the CL scale has been widely implemented in research studies, including both AMYPAD studies and various clinical trials (Fig. 3) [25, 51, 52, 57, 69, 107, 112–114, 132, 136, 138, 146–155].

One of the key advantages of an “absolute” metric of amyloid burden is generalisation of quantitative thresholds across tracers and pipeline implementations. Universal cut-off or threshold values to denote amyloid status can be applied alongside visual reads and in longitudinal multi-centre studies to facilitate inter-centre and inter-tracer comparisons. The CL approach has been validated against neuropathology [148, 149] where CL < 10 correlates with absence of neuritic plaques, CL > 20 specified at least moderate

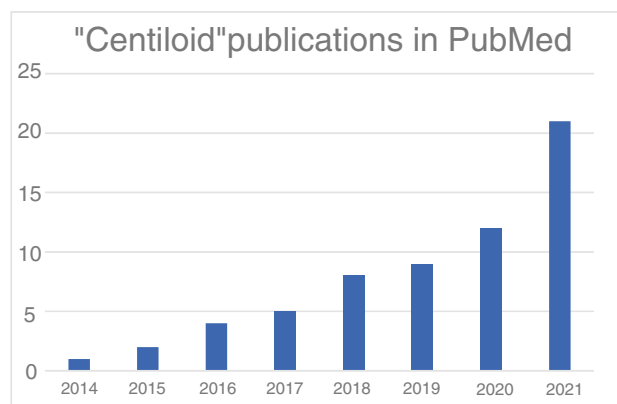


Fig. 3 Bar graph showing the increasing use of CLs in academic publications. The numbers were obtained through a PubMed search for “Centiloid” in all fields on 7th September 2021

Table 1 Conversion equations using the whole cerebellum as reference region applicable to the standard CL processing pipeline for generating CL scores with the most commonly used tracers, adapted from [101]

Tracer	Variance (CL SD) young controls	Variance ratio (tracer SD/PiB SD)	Slope (tracer SUVR to PiB SUVR)	Intercept	R ²	CL equation CL =
[¹⁸ F]Florbetapir [143]	12.0	4.6	0.54	0.5	0.89	175.4*SUVR _{fbp} –182.3
[¹⁸ F]Flutemetamol [52]	5.4	1.54	0.78	0.2	0.95	121.4*SUVR _{flute} –121.2
[¹⁸ F]Florbetaben [136]	6.8	1.96	0.61	0.4	0.96	153.4*SUVR _{fb} –154.9
[¹¹ C]PiB [138]	3.5	n/a	n/a	n/a	n/a	93.7*SUVR _{piB} –94.6

plaque density, and > 50 CL best confirmed both neuropathological and clinicopathological evidence of AD. Clinical studies have also validated thresholds for amyloid PET positive status [25, 132, 146], defined “grey zone” patient cut-offs [107] and derived CL cut-offs to detect early amyloid abnormalities in cognitively unimpaired individuals [69, 150–152]. Predictive models using the CL scale have been developed for calculating rate of cognitive decline in cognitively normal subjects [153–155]. In addition, Hanseeuw et al. [156] found that a CL threshold of 26 in memory clinic patients optimally predicts progression to dementia 6 years after PET.

In clinical trial settings, quantification may be used to identify the optimal window for therapeutic intervention [157]. This is illustrated by the AHEAD 3-45 study, which requires participants to have specific levels of amyloid pathology, either “intermediate” (20–40 CL) or “elevated” (> 40 CL), signifying the added value beyond binary classifications [158]. The CL scale has been used in clinical trial settings to track therapy response measure [111–114, 159, 160], determine strategies for reducing AD prevention trial sample sizes [161], and improve patient selection for trials [48, 162] and could assist in treatment endpoint decisions [51]. Various cut-offs established in the literature are summarised in Fig. 4.

Z-scores

Z-scores represent the number of standard deviations from the mean of a reference or control group and are generally based on SUVr values. It can be calculated for both composite cortical regions, individual regions [97], and at voxel

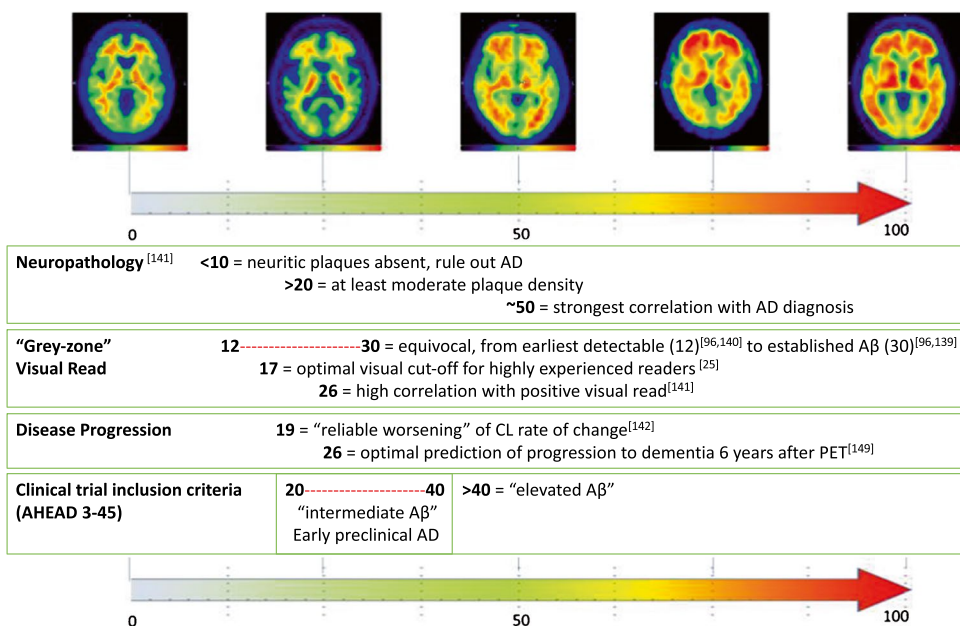
level [58, 163]. Therefore, z-scores are another method for establishing whether a subject’s amyloid deposition should be considered abnormal. Previous work using a classification threshold of $z = 2.0$ demonstrated high concordance with visual read and an autopsy cohort [97]. Based on a set of amyloid negative subjects, an average image (NID_{Ave}) and a standard deviation image (NID_{SD}) are created. The patient scan (Pat) is then compared to this reference database as follows:

$$Pat_{Zscore} = \frac{Pat_{SUVr} - NID_{Ave}}{NID_{SD}}$$

Implementation

Z-scores are widely used in several areas of medical research. In the context of amyloid PET, four of the five commercial software packages covered in this review generate z-scores. One recent study compared the results of two packages with visual assessment, reporting that both software packages provide a high sensitivity and can assist with reporting more complex cases, such as those with atrophy or poor grey-white matter differentiation [164]. Optimal z-score thresholds for amyloid positivity have been established for the pons (1.97) and cerebellar cortex (2.41) as reference regions [165]. These thresholds have been validated against histopathological classification and visual read [97]. Several studies have used z-score maps for predicting and measuring temporal trajectories and patterns of Aβ and tau accumulation in AD [70], where the entorhinal cortex is flagged as

Fig. 4 Summary of the various CL thresholds established in the literature and in use for clinical current clinical trial inclusion



one of earliest areas for tau deposition and medial cortical areas for A β deposits [166–168].

A β load

With the aim of increasing sensitivity for detecting change and therefore statistical power in clinical trials, the A β load metric was developed by Invicro (<https://invicro.com/case-studies/amyloid-load/>) as a novel approach to quantify global A β burden using [^{18}F]florbetapir as the test ligand. In line with CL, PET images are co-registered to a corresponding T1-weighted MRI and transformed to MNI space. The A β load metric is then generated based on spatiotemporal modelling work as a linear combination of two previously defined canonical images: (i) nonspecific binding of [^{18}F]florbetapir and (ii) “A β carrying capacity,” which is the greatest possible A β concentration for a specific region [169]. The final A β load calculation is performed with the MATLAB-implemented “Amyloid^{IQ} algorithm,” which uses both cross-sectional and longitudinal PET and MRI from ADNI to generate a percentage of global A β burden [98, 169].

Implementation

The A β load metric has been implemented for assessing amyloid accumulation in Down’s syndrome [170, 171] and in a multisite analysis of the concordance of visual read and amyloid PET quantification [65], which found 92.5% concordance across 120 scans.

A β index

The A β PET pathology accumulation index does not require an MRI as it is based on a PET-driven principal component analysis (PCA) method [99, 172]. The A β index corresponds to a weighting factor acquired during spatial normalisation of the images to MNI space using a previously described adaptive principal component template [172]. Two principal components are generated using the single value decomposition from SUVr images: (i) the average of the images and (ii) either the specific binding or the elements of discrepancy between A β positive and A β negative scans. A synthetic template is generated using the linear combination of these two principal components, from which a bounded metric between -1 and 1 is generated to define the global A β burden.

Implementation

The A β index has not been widely used to date. Nonetheless, it was recently used in a study comparing visual read and automated methods for amyloid PET processing, where an

optimal cut-off score of -0.36 achieved a sensitivity of 97% based on visual read in 155 elderly controls over a 4.5 year follow up [173].

AMYQ

The most recently developed technique is AMYQ, which is based on similar methodology to the A β index, does not require an MRI scan, and is interchangeable across tracers [100]. As with the A β index, a synthetic amyloid template is generated using PCA and is independent of predefined regions of minimal cortical load or corresponding reference regions for scaling the PET. AMYQ uses the same scale as CL and was recently validated against CL for detecting amyloid positivity (area under curve > 0.94) and for accuracy in differentiating AD dementia patients and controls [100]. AMYQ is yet to be used or validated in further clinical studies.

Comparison of quantitative measures for assessing brain amyloid

The various methods have been summarised for direct comparison in Table 2, and Fig. 5 shows an example of each measure calculated from a subject with high and one with low amyloid uptake.

Regulatory approved tools and research methods for amyloid PET quantification

Various regulatory approved (FDA 510k/CE-marked) software packages currently exist for automated quantification of amyloid PET:

1. Syntermed’s *NeuroQ* (<https://www.syntermed.com/neuroq>) — which generates z -scores and a “cortex-to-whole cerebellum ratio” based on the standard SUVr.
2. Hermes Medical Solutions’ *BRASS* (<https://www.hermesmedical.com/neurology/>) — which generates an SUVr relative to the whole cerebellum and a z -score (≥ 2 in ROI is considered positive) based on a normative database of 80 healthy controls [164].
3. MIM Software’s *MIMneuro* (https://www.mimsoftware.com/nuclear_medicine/mim_neuro) — which uses a standardised PET template registration to generate voxel-based surface projections, regional and mean SUVr, and z -score statistics without the need for an MRI [181]. MIM has also recently implemented the Centiloid scale across multiple tracers.
4. GE Healthcare’s *CortexID* (<https://www.gehealthcare.com/courses/aw-cortex-id>) — which generates SUVr

Table 2 Comparison of the various methods available for amyloid PET quantification

Metric	Units	Basis of measure	Utility/widespread use	Validation	Imaging needs	Strengths	Weaknesses
SUVr	Ratio	Ratio of tracer uptake between a target and reference region	Widely implemented through CE/FDA-approved software	Versus visual read in controls, MCI, and AD patients [173–175] Test-retest [21, 64, 175, 176] Histopathology [19, 97] and CSF [177]	Static PET Structural MRI, although SUVr can be calculated PET only from template ROIs	Easy to calculate across multiple regions Available through CE/FDA-approved software Widely validated against other measures on a variety of clinical populations	Dependent on tracer, reference/target region, and analytical implementation Variability in longitudinal studies [116, 129], resulting in limited power for detecting biological differences
CL	Centiloids (0–100), unbounded	Mean amyloid deposition of young healthy controls (0) to typical AD patients (100)	Increasingly widely used in research and clinical settings, available through CE/FDA-approved software	Against SUVr, and including test-retest [74] Neuropathologically [148, 149, 178] and CSF [147] Positivity threshold validation [146]	Static PET Structural MRI recommended	Universal, tracer independent metric available through CE/FDA-approved software	MRI recommended, although more recent iterations have removed this requirement [96, 145]
Z-score	Standard deviations	Difference from mean of a cognitively healthy population	Widely implemented through CE/FDA-approved software	Widely validated statistical metric for amyloid positivity [58, 97, 109, 164, 179]	Static PET	Widely validated against other measures on a variety of clinical populations Easily interpreted Well known and widely used metric available through CE/FDA-approved software Easy to calculate across multiple regions, easily interpreted	Currently only validated for global/whole brain ROIs rather than regional — not as sensitive to focal uptake as regional measures Reliant on accurate SUVr measurements Dependent on reference/target region and analytical implementation Requires a normative reference database

Table 2 (continued)

Metric	Units	Basis of measure	Utility/widespread use	Validation	Imaging needs	Strengths	Weaknesses
Aβ load	%	Global Aβ burden	Not widely used	Against SUVR [98]	Static [¹⁸ F]florbetapir PET Structural MRI	Larger effect sizes than SUVR — increased power in clinical trials Easily interpreted as a %	Unavailable through CE/FDA-approved software Tracer specific (¹⁸ F]florbetapir), although work is ongoing for other tracers Not yet widely validated
Aβ index	–1, 1	Global Aβ burden/specific binding	Not widely used	Against SUVR, CSF, visual read, and neuropathology [99, 173]	Static [¹⁸ F]florbetapir and [¹⁸ F]flutemetamol [¹⁸ F]florbetaben work is ongoing [180]	Does not require an MRI Interchangeable across [¹⁸ F]florbetapir and [¹⁸ F]flutemetamol PET	Unavailable through CE/FDA-approved software, although planned to be incorporated as part of Hermes Medical Solutions' BRASS software Not yet widely validated or implemented
AMYQ	0–100, unbounded	Global Aβ burden	Not widely used	Against CL and neuropathology [100]	Static PET	Does not require an MRI Interchangeable across tracers Independent of reference and target regions	Unavailable through CE/FDA-approved software Not yet widely validated or implemented

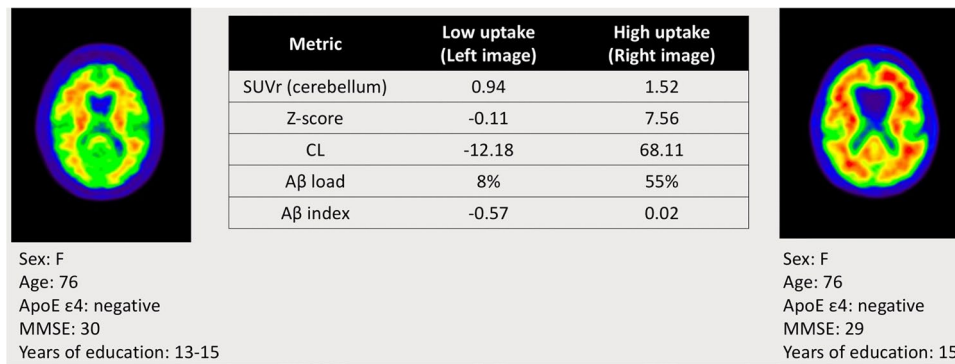


Fig. 5 Example of quantitative metrics computed on two subjects from the AIBL dataset scanned with [^{18}F]flutemetamol. Low amyloid uptake (left image) and high amyloid uptake (right image), including demographics. It was not possible to compute AMYQ due to

the proprietary nature of the software. Abbreviations: mini-mental state examination (MMSE), standardised uptake value ratio (SUVr); amyloid- β (A β)

and z-score surface projection maps of individual patients [97].

- Siemens Healthineers' *Syngo.VIA* (<https://www.siemens-healthineers.com/medical-imaging-it/advanced-visualization-solutions/syngovia>) — which uses positive cut-off value of SUVr ≥ 1.17 and a further threshold of SUVr ≥ 1.08 to assess “identifiable” levels of A β plaques, both of which are derived from previous work [182].
- Qubitech's *Neurocloud PET* (<https://www.qubitech.com/en/solutions/neurocloud-pet/>) — which generates individual SUVr using the whole cerebellum as a reference region.

Other tools are available in research settings, such as PMOD (<https://www.pmod.com/web/?portfolio=CL>), MIAKAT (<https://nmmitools.org/2019/01/01/miakat/>), CapAIBL [183], Evaluation of Brain Amyloidosis (ELBA) [184], and NiftyPET (<https://github.com/NiftyPET/NiftyPET>) [102]. In addition, companies with CE/FDA cleared tools in the radiology AI space have software in development and validation stages, such as ADM diagnostics (<https://admdx.com/>), icometrix (<https://icometrix.com/services>), Cortechs.ai (<https://www.cortechs.ai/products/petquant-2/>), and Combinostics (www.combinostics.com). However, detailed coverage of these tools is beyond the scope of this review as they are not yet approved for clinical use.

Why is amyloid PET quantification valuable and clinically beneficial?

In this review, various methods for automated quantification of amyloid PET measures are presented and discussed. These methods are becoming more widely available and there is a duty of care to the wider dementia community to

increase their visibility and facilitate greater understanding of these methods.

Quantification in clinical practice

Quantification of amyloid PET has shown strong concordance with binary visual assessment in several studies [25, 57, 63, 65, 66, 97, 107, 109, 173, 174, 185]. Amyloid PET tracers available in clinical and research settings have all demonstrated comparable cross-sectional amyloid SUVr results [186–188]. However, there has been no direct head-to-head comparison of the three tracers within the same cohort. As such, the individual effectiveness of each tracer in, for example, assessing an equivocal test set remains to be seen. Other recent studies have found that using quantification alongside visual reads improves diagnostic confidence [33, 36, 38–40, 189], accuracy, and consistency for (i) early detection of amyloid (mild AD, MCI, and controls) [58, 190]; (ii) less experienced readers, i.e. those with visual read accuracy of $\leq 90\%$ [63]; and (iii) more difficult to interpret cases, such as patients with unclear diagnoses or weaker grey-white matter differentiation [57, 109, 164]. However, additional inter-tracer standardisation is required to facilitate multi-centre patient assessment, collaborations, and longitudinal evaluation [191]. More broadly, there remains a need to increase the general understanding of quantitative measures and their diagnostic information. SUVr is the most widely used metric but, as previously mentioned, accurate results are highly dependent on chosen reference region and its delineation [74, 129, 130]. The CL scale could provide a continuous standardised metric that aligns the use of target and reference regions and harmonises the outcome measures [74, 146]. Multiple standardised cut-offs have also been established to progress beyond simple binary stratification, provide prognostic information, and predict cognitive decline (Fig. 4).

Table 3 Overview of current validation requirements in amyloid PET quantification and the associated AMYPAD studies currently underway

What research is still required to validate amyloid PET quantification?	What studies are in place to perform this validation?
Technical validation	
Measure agreement among quantification and visual read across cohorts to assess robustness across populations	Diagnostic and Patient Management Study (DPMS) [50] and Prognostic and Natural History Study (PNHS) [51]
Evaluate the utility and robustness of longitudinal quantification measures	Systematic review (<i>PROSPERO ID: CRD42021254695</i>) updating previous work by Schmidt et al., from 2015 [134]
Calculate the impact of data harmonisation on global CL quantification	Ongoing work presented at AAIC 2020: “Harmonization of Amyloid PET Scans Minimizes the Impact of Reconstruction Parameters on Centiloid Values” [103]
Assess CL stability as a function of pipeline design, reference region selection, cortical target, and image resolution. Provide optimal pipeline for multi-centre studies	Ongoing work presented at AAIC 2021: “Evaluating robustness of the Centiloid scale against variations in amyloid PET image resolution” [194]
Compare static acquisition derived metrics with full quantification derived from dual-time window dynamic imaging	“Parametric imaging of dual-time window [¹⁸ F]flutemetamol and [¹⁸ F]florbetaben studies” [195]. Tertiary outcome of the PNHS; predicting disease progression analyses [51]
Routine clinical use (diagnostic settings)	
Determine clinical utility of amyloid PET quantification using a randomised-controlled trial design	Primary outcome of the DPMS [50]
Formally test if and when quantification approaches support visual assessment of difficult cases	Secondary outcome of the DPMS [50]
Assess the value of regional visual read and quantification in routine clinical settings	Tertiary outcome of the DPMS [50]
Scientific and clinical trial settings	
Assess value of quantification to improve risk stratification and individualised disease trajectory in the earliest stages of AD	Primary outcome of the PNHS [51]

Objective quantification of amyloid burden is imperative now more than ever due to the recent approval of aducanumab (Aduhelm) in the USA and the potential availability of other amyloid targeted therapies. Putting controversies aside, accurate A β measures are essential for prescribing the drug, and future similar drugs, most effectively in clinical practice. For example, prophylactic removal of amyloid may not be suitable for all amyloid positive patients, such as those with dual pathologies and mixed dementia [192]. The aducanumab appropriate use recommendations advocate determination of amyloid status but do not cover when, if ever, treatment should stop or the requirements of a maintenance regimen [193]. In the future, therapy response monitoring with quantitative metrics might be relevant from a perspective of patient burden and health economics. With further research, quantitative amyloid PET could provide universal thresholds alongside visual assessment for deeming treatment as either successful or unsuccessful on a per patient basis, and thereby assisting in the decision to continue or cease treatment. Further work on the clinical benefit of adjunct quantification is encouraged; see Table 3 in “Future directions” for an overview of relevant ongoing AMYPAD studies.

Quantification and prevention trials

In addition to clinical practice, established CL thresholds can also be used to improve clinical trial enrolment [48, 158, 161, 162], assess treatment response [111–114, 159, 160], and, as previously mentioned, potentially guide treatment endpoint decisions. Aducanumab is not an AD dementia panacea and will likely form part of a combined therapy [193, 196–198]. Indeed, there are several ongoing and planned clinical trials of novel anti-amyloid and anti-tau agents. These phase II and III trials are large, multi-centre and multi-tracer with the inclusion of data from different scanners, which have implemented standardised and validated quantitative metrics, such as the CL scale. Furthermore, in clinical trials of multiple active dose and placebo-controlled arms, PET signal changes must be averaged across subjects in each treatment arm, highlighting the value of the CL scale. Quantitative metrics will also be critical in establishing the ideal disease stage for therapeutic intervention and if/when to withdraw a drug [69, 161, 162, 199]. Trials are increasingly enrolling cognitively unimpaired individuals who have started to accumulate regional A β but are still considered “negative” both visually and dichotomously, i.e. preclinical AD [6, 200]. In these cases, visual reading can be challenging but

quantification could automatically flag this “grey-zone” status [153–155, 190, 200].

Regional measures of amyloid burden

Regional estimates of A β deposition measured with PET scanning are a potential advantage over CSF and blood-based biomarkers, which do not convey this valuable information [201]. Recently, the field of AD research has focussed on the value of the topographical distribution and extent of amyloid burden, beyond binary classification of the amyloid status [199, 202, 203]. Studies so far have demonstrated the added value of this information for both disease-modifying therapies [112] and in clinical use, especially during the earliest phases of amyloid accumulation where cognitive symptoms are subtle [38, 110, 204–206]. In these cases, regional assessment has improved detection and there remains a need to reliably quantify this early amyloid pathology as secondary prevention trials, such as the AHEAD 3-45 study, move to treat preclinical AD subjects with low but detectable A β levels [200]. Additionally, there is benefit in improving the prognostic value of amyloid imaging in routine clinical practice, by considering the regional location and extent of pathological load, which could improve subject placement along the AD trajectory [199, 207, 208]. While useful, regional quantification brings an additional challenge where smaller regions are more sensitive to quantification errors and confounding factors, such as partial volume effects and changes in cerebral blood flow.

Possible influence of cerebral blood flow

Quantitative measures remain sensitive to changes in cerebral blood flow (CBF), albeit less of an issue in early stages of dementia [92, 93]. This may reduce the accuracy of longitudinal assessment [134] and acquisitions outside of the predefined time window. This review is broadly targeted to the generalist reader rather than specialists but it is worth noting that other (fully) quantitative approaches do exist. These methods require dynamic PET acquisitions and pharmacokinetic modelling using a plasma or reference tissue input. From these scans, the specific tracer binding can be derived, as changes in physiological factors are accounted for, such as CBF and tracer clearance [93]. However, these measures face a similar dependency on radiotracer and also require a longer dynamic acquisition protocol with complex processing requirements, which limits routine clinical use. Future longitudinal intervention studies could make greater use of dynamic imaging to measure smaller effects but this is much less likely in clinical routine due to time constraints [161]. Dual-phase or dual-time window protocols could be considered instead, as they provide measures of specific tracer binding but with shorter acquisition protocols [105,

106]. Nevertheless, the gain in precision would need to be beneficial to the overall workflow and should not supersede routine scanning otherwise.

Future directions

Across the field, there are several initiatives aiming to assess the direct impact of amyloid PET, both clinically and in terms of health economics. While large projects such as the IDEAS trial and ABIDE study [33] already demonstrated the substantial effect on diagnosis and patient management, more recent outcomes are focussed on how undergoing amyloid PET affects hospitalisation, and therefore medical costs. In addition, differences among racial and ethnic groups are under investigation in the Health & Aging Brain among Latino Elders (HABLE) [209]. The next IDEAS phase aims to address racial disparities by recruiting a diverse cohort of at least 2,000 African American and 2,000 Latino subjects among the planned study population of 7,000 [210]. The IDEAS team recently published their PET-only processing pipeline to support the use of standardised quantitative measures in heterogeneous datasets [211]. These efforts are paramount to optimising the use of amyloid PET quantification in clinical routine and trial settings.

Within this context, the AMYPAD initiative covers several projects on the utility, robustness, and harmonisation of amyloid PET, especially for longitudinal measurements. As a body of work, the planned and current studies encompass the relevant validation necessary to drive greater uptake of quantitative measures in clinic for the benefit of patients worldwide. The ongoing AMYPAD studies aiming to meet these validation requirements are also outlined in Table 3.

Although it is a topic beyond the scope of this paper, quantitative analysis is likely to be complemented by AI-driven analysis techniques in the future. Indeed, various deep learning-based strategies currently exist for amyloid status prediction [212, 213] and SUVR quantification [214], and it will be of great interest to see how techniques such as these develop and contribute to the field.

Limitations

Given that this review focusses on the clinical utility of amyloid PET quantification, it was out of scope to assess amyloid PET vs CSF or plasma amyloid measures, other experimental tracers, or PET imaging measures of neuroinflammation and synaptic density. While the CL scale has been used to assess amyloid and tau PET relationships

and their prognostic value [215–217], discussion of tau PET was also out of scope although it remains a topic of interest. Furthermore, dynamic PET scanning can provide greater precision over static PET but requires longer acquisition time, which limits clinical use, and the overall added value still needs to be determined in different indications. As such, dynamic imaging protocols have not been fully discussed in this review. Finally, it was not possible to compute the AMYQ metric due to the proprietary nature of the software.

Conclusion

In conclusion, several metrics are available to facilitate amyloid PET quantification. Accurate, tracer-independent measurements are needed now more than ever, and use of these methods is increasing. Individual strengths and weaknesses have been presented in this state-of-the-art review. Various recent methods do not require an MRI or a priori reference regions but they do require further validation in multi-centre studies against expert visual rating. The CL method has been widely validated and provides the dementia field with a continuous and universal metric. This method aligns the use of target and reference regions and harmonises the outcome measures. Several studies have validated CL thresholds for capturing the dynamic transition of patients from amyloid negativity to positivity, as well as for measuring disease progression, patient stratification, and prognostic assessment. However, further work is still required to determine threshold validity for longitudinal assessment, treatment endpoint decisions, clinical trial inclusion, optimising therapy intervention time points, and guiding dose selection.

Author contribution All authors contributed to the study conception and design. Material preparation was performed by HP, LC, FH, AB, MS, JDG, and GF. The first draft of the manuscript was written by HP and all authors commented on previous versions of the manuscript. All authors read and approved the final manuscript.

Funding The project leading to this publication has received funding from the Innovative Medicines Initiative 2 Joint Undertaking under grant agreement No 115952. This Joint Undertaking receives the support from the European Union's Horizon 2020 research and innovation programme and EFPIA. This communication reflects the views of the authors and neither IMI nor the European Union and EFPIA are liable for any use that may be made of the information contained herein.

Data availability Not applicable for this review.

Declarations

Ethics approval Not applicable for this review.

Consent to participate Not applicable for this review.

Consent for publication Not applicable for this review.

Competing interests HP, GF, MB, and CB are all employees of GE Healthcare. SB and AS are employees of Life Molecular Imaging GmbH. VG has received funding from the Swiss National Science Foundation (project n. 185028, 188355, and 169876), the Velux Foundation, the Schmidheiny Foundation, and research/teaching support through her institution from Siemens Healthineers, GE Healthcare, Roche, Merck, Cerveau Technologies, and Life Molecular Imaging. FB is a steering committee and iDMC member of studies by Biogen, Merck, Roche, and Eisai. He is a consultant to Roche, Biogen, Merck, IXICO, Jansen, and Combinostics. He has research agreements with Novartis, Merck, Biogen, GE, and Roche and is co-founder of Queen Square Analytics Ltd. His research is sponsored by the NIHR-UCLH Biomedical Research Centre, UK MS Society, MAGNIMS-ECTRIMS, EC-H2020, EC-JU (IMI), and EPSRC.

Open Access This article is licensed under a Creative Commons Attribution 4.0 International License, which permits use, sharing, adaptation, distribution and reproduction in any medium or format, as long as you give appropriate credit to the original author(s) and the source, provide a link to the Creative Commons licence, and indicate if changes were made. The images or other third party material in this article are included in the article's Creative Commons licence, unless indicated otherwise in a credit line to the material. If material is not included in the article's Creative Commons licence and your intended use is not permitted by statutory regulation or exceeds the permitted use, you will need to obtain permission directly from the copyright holder. To view a copy of this licence, visit <http://creativecommons.org/licenses/by/4.0/>.

References

- Scheltens P, De Strooper B, Kivipelto M, et al. Alzheimer's disease. *Lancet*. 2021;397:1577–90. [https://doi.org/10.1016/S0140-6736\(20\)32205-4](https://doi.org/10.1016/S0140-6736(20)32205-4).
- Roberts BR, Lind M, Wagen AZ, et al. Biochemically-defined pools of amyloid- β in sporadic Alzheimer's disease: correlation with amyloid PET. *Brain*. 2017;140:1486–98. <https://doi.org/10.1093/brain/awx057>.
- Jack CR, Bennett DA, Blennow K, et al. NIA-AA research framework: toward a biological definition of Alzheimer's disease. *Alzheimers Dement*. 2018;14:535–62.
- Jack CR, Knopman DS, Jagust WJ, et al. Tracking pathophysiological processes in Alzheimer's disease: an updated hypothetical model of dynamic biomarkers. *Lancet Neurol*. 2013;12:207–16. [https://doi.org/10.1016/S1474-4422\(12\)70291-0](https://doi.org/10.1016/S1474-4422(12)70291-0).
- Dubois B, Feldman HH, Jacova C, et al. Research criteria for the diagnosis of Alzheimer's disease: revising the NINCDS-ADRDA criteria. *Lancet Neurol*. 2007;6:734–46. [https://doi.org/10.1016/S1474-4422\(07\)70178-3](https://doi.org/10.1016/S1474-4422(07)70178-3).
- Dubois B, Feldman HH, Jacova C, et al. Advancing research diagnostic criteria for Alzheimer's disease: the IWG-2 criteria. *Lancet Neurol*. 2014;13:614–29. [https://doi.org/10.1016/S1474-4422\(14\)70090-0](https://doi.org/10.1016/S1474-4422(14)70090-0).
- Dubois B, Villain N, Frisoni GB, et al. Clinical diagnosis of Alzheimer's disease: recommendations of the International Working Group. *Lancet Neurol*. 2021;20:484–96. [https://doi.org/10.1016/S1474-4422\(21\)00066-1](https://doi.org/10.1016/S1474-4422(21)00066-1).
- Jack CR, Bennett DA, Blennow K, et al. A/T/N: an unbiased descriptive classification scheme for Alzheimer disease biomarkers. *Neurology*. 2016;87:539–47. <https://doi.org/10.1212/WNL.0000000000002923>.

9. Jack CR, Thorneau TM, Weigand SD, et al. Prevalence of biologically vs clinically defined Alzheimer spectrum entities using the National Institute on Aging-Alzheimer's Association research framework. *JAMA Neurol.* 2019;76:1174–83. <https://doi.org/10.1001/jamaneurol.2019.1971>.
10. Ingala S, De Boer C, Masselink LA, et al. Application of the ATN classification scheme in a population without dementia: findings from the EPAD cohort. *Alzheimers Dement.* 2021;17:1189–204. <https://doi.org/10.1002/alz.12292>.
11. Altomare D, De Wilde A, Ossenkoppele R, et al. Applying the ATN scheme in a memory clinic population: the ABIDE project. *Neurology.* 2019;93:E1635–46. <https://doi.org/10.1212/WNL.0000000000008361>.
12. Dodich A, Mendes A, Assal F, et al. The A/T/N model applied through imaging biomarkers in a memory clinic. *Eur J Nucl Med Mol Imaging.* 2020;47:247–55. <https://doi.org/10.1007/s00259-019-04536-9>.
13. Soldan A, Pettigrew C, Fagan AM, et al. ATN profiles among cognitively normal individuals and longitudinal cognitive outcomes. *Neurology.* 2019;92:E1567–79. <https://doi.org/10.1212/WNL.0000000000007248>.
14. Mattsson N, Carrillo MC, Dean RA, et al. Revolutionizing Alzheimer's disease and clinical trials through biomarkers. *Alzheimer's Dement Diagnosis. Assess Dis Monit.* 2015;1:412–9. <https://doi.org/10.1016/j.dadm.2015.09.001>.
15. Jagust W. Is amyloid- β harmful to the brain? Insights from human imaging studies. *Brain.* 2016;139:23–30. <https://doi.org/10.1093/brain/awv326>.
16. Hardy J, Allsop D. Amyloid deposition as the central event in the aetiology of Alzheimer's disease. *Trends Pharmacol Sci.* 1991;12:383–8. [https://doi.org/10.1016/0165-6147\(91\)90609-V](https://doi.org/10.1016/0165-6147(91)90609-V).
17. Hardy JA, Higgins GA. Alzheimer's disease: the amyloid cascade hypothesis. *Science (80-)* 256:184–185. 1992. <https://doi.org/10.1126/science.1566067>.
18. Villemagne VL, Barkhof F, Garibotto V, et al. Molecular imaging approaches in dementia. *Radiology.* 2021;298:517–30. <https://doi.org/10.1148/radiol.202000028>.
19. Clark CM, Pontecorvo MJ, Beach TG, et al. Cerebral PET with florbetapir compared with neuropathology at autopsy for detection of neuritic amyloid- β plaques: a prospective cohort study. *Lancet Neurol.* 2012;11:669–78. [https://doi.org/10.1016/S1474-4422\(12\)70142-4](https://doi.org/10.1016/S1474-4422(12)70142-4).
20. Salloway S, Gamez JE, Singh U, et al. Performance of [18F]flutemetamol amyloid imaging against the neuritic plaque component of CERAD and the current (2012) NIA-AA recommendations for the neuropathologic diagnosis of Alzheimer's disease. *Alzheimer's Dement Diagnosis. Assess Dis Monit.* 2017;9:25–34. <https://doi.org/10.1016/j.dadm.2017.06.001>.
21. Sabri O, Sabbagh MN, Seibyl J, et al. Florbetaben PET imaging to detect amyloid beta plaques in Alzheimer's disease: phase 3 study. *Alzheimers Dement.* 2015;11:964–74. <https://doi.org/10.1016/j.jalz.2015.02.004>.
22. Klunk WE, Engler H, Nordberg A, et al. Imaging brain amyloid in Alzheimer's disease with Pittsburgh Compound-B. *Ann Neurol.* 2004;55:306–19. <https://doi.org/10.1002/ana.20009>.
23. Rowe CC, Pejoska S, Mulligan RS, et al. Head-to-head comparison of 11C-PiB and 18F-AZD4694 (NAV4694) for β -amyloid imaging in aging and dementia. *J Nucl Med.* 2013;54:880–6. <https://doi.org/10.2967/jnumed.112.114785>.
24. Alongi P, Chiaravallotti A, Berti V, et al. Amyloid PET in the diagnostic workup of neurodegenerative disease. *Clin Transl Imaging.* 2021;9:383–97. <https://doi.org/10.1007/s40336-021-00428-x>.
25. Collij LE, Salvadó G, Shekari M, et al. Visual assessment of [18F]flutemetamol PET images can detect early amyloid pathology and grade its extent. *Eur J Nucl Med Mol Imaging.* 2021;48:2169–82. <https://doi.org/10.1007/s00259-020-05174-2>.
26. Hattori N, Sherwin P, Farrar G. Initial physician experience with [18F]flutemetamol amyloid PET imaging following availability for routine clinical use in Japan. *J Alzheimer's Dis Reports.* 2020;4:165–74. <https://doi.org/10.3233/adr-190150>.
27. Buckley CJ, Sherwin PF, Smith APL, et al. Validation of an electronic image reader training programme for interpretation of [18F]flutemetamol β -amyloid PET brain images. *Nucl Med Commun.* 2017;38:234–41. <https://doi.org/10.1097/MNM.0000000000000633>.
28. Seibyl J, Catafau AM, Barthel H, et al. Impact of training method on the robustness of the visual assessment of 18F-florbetaben PET scans: results from a phase-3 study. *J Nucl Med.* 2016;57:900–6. <https://doi.org/10.2967/jnumed.115.161927>.
29. Pontecorvo MJ, Siderowf A, Dubois B, et al. Effectiveness of florbetapir PET imaging in changing patient management. *Dement Geriatr Cogn Disord.* 2017;44:129–43. <https://doi.org/10.1159/000478007>.
30. Paghera B, Altomare D, Peli A, et al. Comparison of visual criteria for amyloid-pet reading: could criteria merging reduce inter-rater variability? *Q J Nucl Med Mol Imaging.* 2021;64:414–21. <https://doi.org/10.23736/S1824-4785.19.03124-8>.
31. Bischof GN, Bartenstein P, Barthel H, et al. Toward a universal readout for 18F-labeled amyloid tracers: the CAPTAINS study. *J Nucl Med.* 2021;62:999–1005. <https://doi.org/10.2967/jnumed.120.250290>.
32. Chiotis K, Saint-Aubert L, Boccardi M, et al. Clinical validity of increased cortical uptake of amyloid ligands on PET as a biomarker for Alzheimer's disease in the context of a structured 5-phase development framework. *Neurobiol Aging.* 2017;52:214–27. <https://doi.org/10.1016/j.neurobiolaging.2016.07.012>.
33. De Wilde A, Van Der Flier WM, Pelkmans W, et al. Association of amyloid positron emission tomography with changes in diagnosis and patient treatment in an unselected memory clinic cohort: the ABIDE project. *JAMA Neurol.* 2018;75:1062–70. <https://doi.org/10.1001/jamaneurol.2018.1346>.
34. Rabinovici GD, Gatsonis C, Apgar C, et al. Association of amyloid positron emission tomography with subsequent change in clinical management among Medicare beneficiaries with mild cognitive impairment or dementia. *JAMA - J Am Med Assoc.* 2019;321:1286–94. <https://doi.org/10.1001/jama.2019.2000>.
35. Fantoni ER, Chalkidou A, O'Brien JT, et al. A systematic review and aggregated analysis on the impact of amyloid PET brain imaging on the diagnosis, diagnostic confidence, and management of patients being evaluated for Alzheimer's disease. *J Alzheimers Dis.* 2018;63:783–96. <https://doi.org/10.3233/JAD-171093>.
36. Barthel H, Sabri O. Clinical use and utility of amyloid imaging. *J Nucl Med.* 2017;58:1711–7. <https://doi.org/10.2967/jnumed.116.185017>.
37. Grundman M, Johnson KA, Lu M, et al. Effect of amyloid imaging on the diagnosis and management of patients with cognitive decline: impact of appropriate use criteria. *Dement Geriatr Cogn Disord.* 2016;41:80–92. <https://doi.org/10.1159/000441139>.
38. Zwan MD, Bouwman FH, Konijnenberg E, et al. Diagnostic impact of [18F]flutemetamol PET in early-onset dementia. *Alzheimers Res Ther.* 2017;9. <https://doi.org/10.1186/s13195-016-0228-4>.
39. Schipke CG, Peters O, Heuser I, et al. Impact of beta-amyloid-specific florbetaben pet imaging on confidence in early diagnosis of Alzheimer's disease. *Dement Geriatr Cogn Disord.* 2012;33:416–22. <https://doi.org/10.1159/000339367>.

40. Zannas AS, Doraiswamy PM, Shpanskaya KS, et al. Impact of 18F-florbetapir PET imaging of β -amyloid neuritic plaque density on clinical decision-making. *Neurocase*. 2014;20:466–73. <https://doi.org/10.1080/13554794.2013.791867>.
41. Johnson KA, Minoshima S, Bohnen NI, et al. Appropriate use criteria for amyloid PET: a report of the Amyloid Imaging Task Force, the Society of Nuclear Medicine and Molecular Imaging, and the Alzheimer's Association. *Alzheimers Dement*. 2013;9. <https://doi.org/10.1016/j.jalz.2013.01.002>.
42. Altomare D, Ferrari C, Festari C, et al. Quantitative appraisal of the Amyloid Imaging Taskforce appropriate use criteria for amyloid-PET. *Alzheimers Dement*. 2018;14:1088–98. <https://doi.org/10.1016/j.jalz.2018.02.022>.
43. Brooks DJ. Imaging amyloid in Parkinson's disease dementia and dementia with Lewy bodies with positron emission tomography. *Mov Disord*. 2009;24:S742–7. <https://doi.org/10.1002/mds.22581>.
44. Gomperts SN, Rentz DM, Moran E, et al. Imaging amyloid deposition in Lewy body diseases. *Neurology*. 2008;71:903–10. <https://doi.org/10.1212/01.wnl.0000326146.60732.d6>.
45. Mueller SG, Weiner MW, Thal LJ, et al. Ways toward an early diagnosis in Alzheimer's disease: the Alzheimer's Disease Neuroimaging Initiative (ADNI). *Alzheimers Dement*. 2005;1:55–66. <https://doi.org/10.1016/j.jalz.2005.06.003>.
46. Jagust WJ, Landau SM, Koeppe RA, et al. The Alzheimer's disease neuroimaging initiative 2 PET core: 2015. *Alzheimers Dement*. 2015;11:757–71. <https://doi.org/10.1016/j.jalz.2015.05.001>.
47. Jagust WJ, Bandy D, Chen K, et al. The Alzheimer's Disease Neuroimaging Initiative positron emission tomography core. *Alzheimers Dement*. 2010;6:221–9. <https://doi.org/10.1016/j.jalz.2010.03.003>.
48. Weiner MW, Veitch DP, Aisen PS, et al. The Alzheimer's Disease Neuroimaging Initiative 3: continued innovation for clinical trial improvement. *Alzheimers Dement*. 2017;13:561–71. <https://doi.org/10.1016/j.jalz.2016.10.006>.
49. Ellis KA, Bush AI, Darby D, et al. The Australian Imaging, Biomarkers and Lifestyle (AIBL) study of aging: methodology and baseline characteristics of 1112 individuals recruited for a longitudinal study of Alzheimer's disease. *Int Psychogeriatr*. 2009;21:672–87. <https://doi.org/10.1017/S1041610209009405>.
50. Frisoni GB, Barkhof F, Altomare D, et al. AMYPAD diagnostic and patient management study: rationale and design. *Alzheimers Dement*. 2019;15:388–99. <https://doi.org/10.1016/j.jalz.2018.09.003>.
51. Lopes Alves I, Collij LE, Altomare D, et al. Quantitative amyloid PET in Alzheimer's disease: the AMYPAD prognostic and natural history study. *Alzheimers Dement*. 2020;16:750–8. <https://doi.org/10.1002/alz.12069>.
52. Battle MR, Pillay LC, Lowe VJ, et al. Centiloid scaling for quantification of brain amyloid with [18F]flutemetamol using multiple processing methods. *EJNMMI Res*. 2018;8:1–11. <https://doi.org/10.1186/s13550-018-0456-7>.
53. Teipel SJ, Dyrba M, Vergallo A, et al. Partial volume correction increases the sensitivity of 18F-florbetapir-positron emission tomography for the detection of early stage amyloidosis. *Front Aging Neurosci*. 2021;13:846. <https://doi.org/10.3389/fnagi.2021.748198>.
54. Shidahara M, Thomas BA, Okamura N, et al. A comparison of five partial volume correction methods for tau and amyloid PET imaging with [18F]THK5351 and [11C]PIB. *Ann Nucl Med*. 2017;31:563–9. <https://doi.org/10.1007/s12149-017-1185-0>.
55. Schwarz CG, Gunter JL, Lowe VJ, et al. A comparison of partial volume correction techniques for measuring change in serial amyloid PET SUVR. *J Alzheimers Dis*. 2019;67:181–95. <https://doi.org/10.3233/JAD-180749>.
56. Rinne JO, Wong DF, Wolk DA, et al. Flutemetamol PET imaging and cortical biopsy histopathology for fibrillar amyloid β detection in living subjects with normal pressure hydrocephalus: pooled analysis of four studies. *Acta Neuropathol*. 2012;124:833–45. <https://doi.org/10.1007/s00401-012-1051-z>.
57. Matsuda H, Ito K, Ishii K, et al. Quantitative evaluation of 18F-flutemetamol PET in patients with cognitive impairment and suspected Alzheimer's disease: a multicenter study. *Front Neurol* 11. 2021. <https://doi.org/10.3389/fneur.2020.578753>.
58. Akamatsu G, Ikari Y, Ohnishi A, et al (2019) Voxel-based statistical analysis and quantification of amyloid PET in the Japanese Alzheimer's disease neuroimaging initiative (J-ADNI) multi-center study. *EJNMMI Res* 2019, 9. <https://doi.org/10.1186/s13550-019-0561-2>
59. Chételat G, Arbizu J, Barthel H, et al. Amyloid-PET and 18F-FDG-PET in the diagnostic investigation of Alzheimer's disease and other dementias. *Lancet Neurol*. 2020;19:951–62. [https://doi.org/10.1016/S1474-4422\(20\)30314-8](https://doi.org/10.1016/S1474-4422(20)30314-8).
60. Ossenkoppele R, Jansen WJ, Rabinovici GD, et al. Prevalence of amyloid PET positivity in dementia syndromes: a meta-analysis. *Jama*. 2015;313:1939–49. <https://doi.org/10.1001/jama.2015.4669>.
61. Van Der Flier WM, Scheltens P. Amsterdam dementia cohort: performing research to optimize care. *J Alzheimers Dis*. 2018;62:1091–111. <https://doi.org/10.3233/JAD-170850>.
62. Fantoni E, Collij L, Alves IL, et al. The spatial-temporal ordering of amyloid pathology and opportunities for PET imaging. *J Nucl Med*. 2020;61:166–71. <https://doi.org/10.2967/jnumed.119.235879>.
63. Pontecorvo MJ, Arora AK, Devine M, et al. Quantitation of PET signal as an adjunct to visual interpretation of florbetapir imaging. *Eur J Nucl Med Mol Imaging*. 2017;44:825–37. <https://doi.org/10.1007/s00259-016-3601-4>.
64. Joshi AD, Pontecorvo MJ, Clark CM, et al. Performance characteristics of amyloid PET with florbetapir F 18 in patients with Alzheimer's disease and cognitively normal subjects. *J Nucl Med*. 2012;53:378–84. <https://doi.org/10.2967/jnumed.111.090340>.
65. Bucci M, Savitcheva I, Farrar G, et al. A multisite analysis of the concordance between visual image interpretation and quantitative analysis of [18F]flutemetamol amyloid PET images. *Eur J Nucl Med Mol Imaging*. 2021;48:2183–99. <https://doi.org/10.1007/s00259-021-05311-5>.
66. Yamane T, Ishii K, Sakata M, et al. Inter-rater variability of visual interpretation and comparison with quantitative evaluation of 11C-PiB PET amyloid images of the Japanese Alzheimer's Disease Neuroimaging Initiative (J-ADNI) multicenter study. *Eur J Nucl Med Mol Imaging*. 2017;44:850–7. <https://doi.org/10.1007/s00259-016-3591-2>.
67. Aisen PS, Cummings J, Doody R, et al. The future of anti-amyloid trials. *J Prev Alzheimer's Dis*. 2020;7:146–51. <https://doi.org/10.14283/jpad.2020.24>.
68. Blennow K, Zetterberg H. Amyloid and tau biomarkers in CSF. *J Prev Alzheimer's Dis*. 2015;2:1–5. <https://doi.org/10.14283/jpad.2015.41>.
69. Milà-Alomà M, Salvadó G, Shekari M, et al. Comparative analysis of different definitions of amyloid- β positivity to detect early downstream pathophysiological alterations in preclinical Alzheimer. *J Prev Alzheimer's Dis*. 2021;8:68–77. <https://doi.org/10.14283/jpad.2020.51>.
70. Camus V, Payoux P, Barré L, et al. Using PET with 18F-AV-45 (florbetapir) to quantify brain amyloid load in a clinical environment. *Eur J Nucl Med Mol Imaging*. 2012;39:621–31. <https://doi.org/10.1007/s00259-011-2021-8>.
71. Guerra UP, Nobili FM, Padovani A, et al. Recommendations from the Italian Interdisciplinary Working Group (AIMN, AIP,

- SINDEM) for the utilization of amyloid imaging in clinical practice. *Neurol Sci.* 2015;36:1075–81. <https://doi.org/10.1007/s10072-015-2079-3>.
72. Kobylecki C, Langheinrich T, Hinz R, et al. 18F-florbetapir PET in patients with frontotemporal dementia and Alzheimer disease. *J Nucl Med.* 2015;56:386–91. <https://doi.org/10.2967/jnumed.114.147454>.
73. Daniela P, Orazio S, Alessandro P, et al (2014) A survey of FDG- and amyloid-PET imaging in dementia and grade analysis. *Biomed Res Int* 2014;. <https://doi.org/10.1155/2014/785039>
74. Klunk WE, Koeppe RA, Price JC, et al. The Centiloid project: standardizing quantitative amyloid plaque estimation by PET. *Alzheimers Dement.* 2015;11:1–15.e4. <https://doi.org/10.1016/j.jalz.2014.07.003>.
75. Hedderich DM, Dieckmeyer M, Andrisan T, et al. Normative brain volume reports may improve differential diagnosis of dementing neurodegenerative diseases in clinical practice. *Eur Radiol.* 2020;30:2821–9. <https://doi.org/10.1007/s00330-019-06602-0>.
76. Pemberton HG, Goodkin O, Prados F, et al. Automated quantitative MRI volumetry reports support diagnostic interpretation in dementia: a multi-rater, clinical accuracy study. *Eur Radiol.* 2021;31:5312–23. <https://doi.org/10.1007/s00330-020-07455-8>.
77. Vernooij MW, Jaspers B, Steketee R, et al. Automatic normative quantification of brain tissue volume to support the diagnosis of dementia: a clinical evaluation of diagnostic accuracy. *NeuroImage Clin.* 2018;20:374–9. <https://doi.org/10.1016/j.nicl.2018.08.004>.
78. Pemberton HG, Zaki LAM, Goodkin O, et al. Technical and clinical validation of commercial automated volumetric MRI tools for dementia diagnosis—a systematic review. *Neuroradiology.* 2021;63:1773–89. <https://doi.org/10.1007/s00234-021-02746-3>.
79. Ross DE, Ochs AL, Seabaugh JM, Shrader CR. Man versus machine: comparison of radiologists' interpretations and NeuroQuantspi® volumetric analyses of brain MRIs in patients with traumatic brain injury. *J Neuropsychiatr Clin Neurosci.* 2013;25:32–9. <https://doi.org/10.1176/appi.neuropsych.11120377>.
80. Ross DE, Ochs AL, Desmit ME, et al. Man versus machine part 2: comparison of radiologists' interpretations and neuroquant measures of brain asymmetry and progressive atrophy in patients with traumatic brain injury. *J Neuropsychiatr Clin Neurosci.* 2015;27:147–52. <https://doi.org/10.1176/appi.neuropsych.1304088>.
81. Vos SB, Winston GP, Goodkin O, et al. Hippocampal profiling: localized magnetic resonance imaging volumetry and T2 relaxometry for hippocampal sclerosis. *Epilepsia.* 2020;61:297–309. <https://doi.org/10.1111/epi.16416>.
82. Louis S, Morita-Sherman M, Jones S, et al. Hippocampal sclerosis detection with neuroquant compared with neuroradiologists. *Am J Neuroradiol.* 2020;41:591–7. <https://doi.org/10.3174/AJNR.A6454>.
83. Mettenburg JM, Branstetter BF, Wiley CA, et al. Improved detection of subtle mesial temporal sclerosis: validation of a commercially available software for automated segmentation of hippocampal volume. *Am J Neuroradiol.* 2019;40:440–5. <https://doi.org/10.3174/ajnr.A5966>.
84. Goodkin O, Pemberton HG, Vos SB, et al. Clinical evaluation of automated quantitative MRI reports for assessment of hippocampal sclerosis. *Eur Radiol.* 2021;31:34–44. <https://doi.org/10.1007/s00330-020-07075-2>.
85. Hov MR, Røislien J, Lindner T, et al. Stroke severity quantification by critical care physicians in a mobile stroke unit. *Eur J Emerg Med.* 2019;26:194–8. <https://doi.org/10.1097/MEJ.0000000000000529>.
86. Mokli Y, Pfaff J, dos Santos DP, et al. Computer-aided imaging analysis in acute ischemic stroke—background and clinical applications. *Neurol Res Pract.* 2019;1:1–13. <https://doi.org/10.1186/s42466-019-0028-y>.
87. De Witt Hamer PC, Hendriks EJ, Mandonnet E, et al. Resection probability maps for quality assessment of glioma surgery without brain location bias. *PLoS One.* 2013;8. <https://doi.org/10.1371/journal.pone.0073353>.
88. Müller DMJ, Robe PA, Ardon H, et al. Quantifying eloquent locations for glioblastoma surgery using resection probability maps. *J Neurosurg.* 2021;134:1091–101. <https://doi.org/10.3171/2020.1.JNS193049>.
89. Niemantsverdriet E, Ribbens A, Bastin C, et al. A retrospective Belgian multi-center MRI biomarker study in Alzheimer's disease (REMEMBER). *J Alzheimers Dis.* 2018;63:1509–22. <https://doi.org/10.3233/JAD-171140>.
90. Smeets D, Ribbens A, Sima DM, et al. Reliable measurements of brain atrophy in individual patients with multiple sclerosis. *Brain Behav.* 2016;6. <https://doi.org/10.1002/brb3.518>.
91. Goodkin O, Prados F, Vos SB, et al (2021) FLAIR-only joint volumetric analysis of brain lesions and atrophy in clinically isolated syndrome (CIS) suggestive of multiple sclerosis. *NeuroImage Clin* 29;. <https://doi.org/10.1016/j.nicl.2020.102542>
92. Cselényi Z, Farde L. Quantification of blood flow-dependent component in estimates of beta-amyloid load obtained using quasi-steady-state standardized uptake value ratio. *J Cereb Blood Flow Metab.* 2015;35:1485–93. <https://doi.org/10.1038/jcbfm.2015.66>.
93. Heeman F, Yaqub M, Lopes Alves I, et al. Simulating the effect of cerebral blood flow changes on regional quantification of [18F]flutemetamol and [18F]florbetaben studies. *J Cereb Blood Flow Metab.* 2021;41:579–89. <https://doi.org/10.1177/0271678X20918029>.
94. Lammertsma AA. Forward to the past: the case for quantitative PET imaging. *J Nucl Med.* 2017;58:1019–24. <https://doi.org/10.2967/jnumed.116.188029>.
95. Lopresti BJ, Klunk WE, Mathis CA, et al. Simplified quantification of Pittsburgh compound B amyloid imaging PET studies: a comparative analysis. *J Nucl Med.* 2005;46:1959–72.
96. Bourgeat P, Doré V, Doecke J, et al. Non-negative matrix factorisation improves Centiloid robustness in longitudinal studies. *Neuroimage.* 2021;226. <https://doi.org/10.1016/j.neuroimage.2020.117593>.
97. Thurjell L, Lilja J, Lundqvist R, et al. Automated quantification of 18F-flutemetamol PET activity for categorizing scans as negative or positive for brain amyloid: concordance with visual image reads. *J Nucl Med.* 2014;55:1623–8. <https://doi.org/10.2967/jnumed.114.142109>.
98. Whittington A, Gunn RN. Amyloid load: a more sensitive biomarker for amyloid imaging. *J Nucl Med.* 2019;60:536–40. <https://doi.org/10.2967/jnumed.118.210518>.
99. Leuzy A, Lilja J, Buckley CJ, et al. Derivation and utility of an Aβ-PET pathology accumulation index to estimate Aβ load. *Neurology.* 2020;95:e2834–44. <https://doi.org/10.1212/WNL.0000000000001031>.
100. Pegueroles J, Montal V, Bejanin A, et al. AMYQ: an index to standardize quantitative amyloid load across PET tracers. *Alzheimers Dement.* 2021;17:1499–508. <https://doi.org/10.1002/alz.12317>.
101. Krishnadas N, Villemagne VL, Doré V, Rowe CC. Advances in brain amyloid imaging. *Semin Nucl Med.* 2021;51:241–52. <https://doi.org/10.1053/j.semnuclmed.2020.12.005>.
102. Markiewicz PJ, Ehrhardt MJ, Erlandsson K, et al. NiftyPET: a high-throughput software platform for high quantitative accuracy and precision PET imaging and analysis. *Neuroinformatics.* 2018;16:95–115. <https://doi.org/10.1007/s12021-017-9352-y>.

103. Shekari M, Niñerola-Baizán A, Salvadó G, et al. Harmonization of amyloid PET scans minimizes the impact of reconstruction parameters on centiloid values. *Alzheimers Dement*. 2020;16:e045294. <https://doi.org/10.1002/alz.045294>.
104. Bourgeat P, Doré V, Fripp J, et al. Implementing the centiloid transformation for 11C-PiB and β -amyloid 18F-PET tracers using CapAIBL. *Neuroimage*. 2018;183:387–93. <https://doi.org/10.1016/j.neuroimage.2018.08.044>.
105. Heeman F, Yaqub M, Alves IL, et al. Optimized dual-time-window protocols for quantitative [18F]flutemetamol and [18F]florbetaben PET studies. *EJNMMI Res*. 2019;9:1–14. <https://doi.org/10.1186/s13550-019-0499-4>.
106. Bullich S, Barthel H, Koglin N, et al. Validation of noninvasive tracer kinetic analysis of 18 F-Florbetaben PET using a dual-time-window acquisition protocol. *J Nucl Med*. 2018;59:1104–10. <https://doi.org/10.2967/jnumed.117.200964>.
107. Bullich S, Roé-Vellvé N, Marquíé M, et al. Early detection of amyloid load using 18F-florbetaben PET. *Alzheimers Res Ther*. 2021;13. <https://doi.org/10.1186/s13195-021-00807-6>.
108. Bullich S, Salvadó G, Alves IL, et al. Converging evidence for a “gray-zone” of amyloid burden and its relevance. *Alzheimers Dement*. 2020;16:e044786. <https://doi.org/10.1002/alz.044786>.
109. Leuzy A, Savitcheva I, Chiotis K, et al (2019) Clinical impact of [18F]flutemetamol PET among memory clinic patients with an unclear diagnosis. *Eur J Nucl Med Mol Imaging* 46:. <https://doi.org/10.1007/s00259-019-04297-5>
110. Collij LE, Mastenbroek SE, Salvadó G, et al. Regional amyloid accumulation predicts memory decline in initially cognitively unimpaired individuals. *Alzheimer’s Dement Diagnosis. Assess Dis Monit*. 2021;13:e12216. <https://doi.org/10.1002/dad2.12216>.
111. Roberts C, Kaplow J, Giroux M, et al. Amyloid and APOE Status of Screened Subjects in the Elenbecestat MissionAD Phase 3 Program. *J Prev Alzheimer’s Dis*. 2021;8:218–23. <https://doi.org/10.14283/jpad.2021.4>.
112. Mintun MA, Lo AC, Duggan Evans C, et al. Donanemab in early Alzheimer’s disease. *N Engl J Med*. 2021;384:1691–704. <https://doi.org/10.1056/nejmoa2100708>.
113. Klein G, Delmar P, Kerchner GA, et al. Thirty-six-month amyloid positron emission tomography results show continued reduction in amyloid burden with subcutaneous gantenerumab. *J Prev Alzheimer’s Dis*. 2021;8:3–6. <https://doi.org/10.14283/jpad.2020.68>.
114. Klein G, Delmar P, Voyle N, et al. Gantenerumab reduces amyloid- β plaques in patients with prodromal to moderate Alzheimer’s disease: a PET substudy interim analysis. *Alzheimers Res Ther*. 2019;11. <https://doi.org/10.1186/s13195-019-0559-z>.
115. Lammertsma AA, Hume SP. Simplified reference tissue model for PET receptor studies. *Neuroimage*. 1996;4:153–8. <https://doi.org/10.1006/nimg.1996.0066>.
116. Landau SM, Fero A, Baker SL, et al. Measurement of longitudinal β -amyloid change with 18F-florbetapir PET and standardized uptake value ratios. *J Nucl Med*. 2015;56:567–74. <https://doi.org/10.2967/jnumed.114.148981>.
117. Bullich S, Villemagne VL, Catafau AM, et al. Optimal reference region to measure longitudinal amyloid-b change with 18F-florbetaben PET. *J Nucl Med*. 2017;58:1300–6. <https://doi.org/10.2967/jnumed.116.187351>.
118. Cho SH, Choe YS, Park S, et al (2020) Appropriate reference region selection of 18F-florbetaben and 18F-flutemetamol beta-amyloid PET expressed in Centiloid. *Sci Rep* 10:. <https://doi.org/10.1038/s41598-020-70978-z>
119. Mormino EC, Kluth JT, Madison CM, et al. Episodic memory loss is related to hippocampal-mediated β -amyloid deposition in elderly subjects. *Brain*. 2009;132:1310–23. <https://doi.org/10.1093/brain/awn320>.
120. Fleisher AS, Chen K, Liu X, et al. Apolipoprotein E ϵ 4 and age effects on florbetapir positron emission tomography in healthy aging and Alzheimer disease. *Neurobiol Aging*. 2013;34:1–12. <https://doi.org/10.1016/j.neurobiolaging.2012.04.017>.
121. Kinahan PE, Fletcher JW. Positron emission tomography-computed tomography standardized uptake values in clinical practice and assessing response to therapy. *Semin Ultrasound, CT MRI*. 2010;31:496–505. <https://doi.org/10.1053/j.sult.2010.10.001>.
122. Honig LS, Vellas B, Woodward M, et al. Trial of solanezumab for mild dementia due to Alzheimer’s disease. *N Engl J Med*. 2018;378:321–30. <https://doi.org/10.1056/nejmoa1705971>.
123. Relkin NR, Thomas RG, Rissman RA, et al. A phase 3 trial of IV immunoglobulin for Alzheimer disease. *Neurology*. 2017;88:1768–75. <https://doi.org/10.1212/WNL.00000000000003904>.
124. Liu E, Schmidt ME, Margolin R, et al. Amyloid- β 11C-PiB-PET imaging results from 2 randomized bapineuzumab phase 3 AD trials. *Neurology*. 2015;85:692–700. <https://doi.org/10.1212/WNL.0000000000001877>.
125. Salloway S, Sperling R, Fox NC, et al. Two phase 3 trials of bapineuzumab in mild-to-moderate Alzheimer’s disease. *N Engl J Med*. 2014;370:322–33. <https://doi.org/10.1056/nejmoa1304839>.
126. Doody RS, Raman R, Farlow M, et al. A phase 3 trial of semagacestat for treatment of Alzheimer’s disease. *N Engl J Med*. 2013;369:341–50. <https://doi.org/10.1056/nejmoa1210951>.
127. Doody RS, Thomas RG, Farlow M, et al. Phase 3 trials of solanezumab for mild-to-moderate Alzheimer’s disease. *N Engl J Med*. 2014;370:311–21. <https://doi.org/10.1056/nejmoa1312889>.
128. Ostrowitzki S, Lasser RA, Dorflinger E, et al. A phase III randomized trial of gantenerumab in prodromal Alzheimer’s disease. *Alzheimers Res Ther*. 2017;9. <https://doi.org/10.1186/s13195-017-0318-y>.
129. Tryputsen V, Dibernardo A, Samtani M, et al. Optimizing regions-of-interest composites for capturing treatment effects on brain amyloid in clinical trials. *J Alzheimers Dis*. 2015;43:809–21. <https://doi.org/10.3233/JAD-131979>.
130. Landau SM, Thomas BA, Thurfjell L, et al. Amyloid PET imaging in Alzheimer’s disease: a comparison of three radiotracers. *Eur J Nucl Med Mol Imaging*. 2014;41:1398–407. <https://doi.org/10.1007/s00259-014-2753-3>.
131. Kolinger GD, Garcia DV, Willemsen ATM, et al. Amyloid burden quantification depends on PET and MR image processing methodology. *PLoS One*. 2021;16:e0248122. <https://doi.org/10.1371/journal.pone.0248122>.
132. Jack CR, Wiste HJ, Weigand SD, et al. Defining imaging biomarker cut points for brain aging and Alzheimer’s disease. *Alzheimers Dement*. 2017;13:205–16. <https://doi.org/10.1016/j.jalz.2016.08.005>.
133. Su Y, Blazey TM, Snyder AZ, et al. Partial volume correction in quantitative amyloid imaging. *Neuroimage*. 2015;107:55–64. <https://doi.org/10.1016/j.neuroimage.2014.11.058>.
134. Schmidt ME, Chiao P, Klein G, et al. The influence of biological and technical factors on quantitative analysis of amyloid PET: points to consider and recommendations for controlling variability in longitudinal data. *Alzheimers Dement*. 2015;11:1050–68. <https://doi.org/10.1016/j.jalz.2014.09.004>.
135. Schwarz CG, Tosakulwong N, Senjem ML, et al. Considerations for performing level-2 centiloid transformations for amyloid PET SUVR values. *Sci Rep*. 2018;8. <https://doi.org/10.1038/s41598-018-25459-9>.
136. Rowe CC, Doré V, Jones G, et al. 18F-florbetaben PET beta-amyloid binding expressed in Centiloids. *Eur J Nucl Med Mol Imaging*. 2017;44:2053–9. <https://doi.org/10.1007/s00259-017-3749-6>.







137. Leuzy A, Chiotis K, Hasselbalch SG, et al. Pittsburgh compound B imaging and cerebrospinal fluid amyloid- β in a multicentre European memory clinic study. *Brain*. 2016;139:2540–53. <https://doi.org/10.1093/brain/aww160>.
138. Rowe CC, Jones G, Dore V, et al. Standardized expression of 18F-NAV4694 and 11C-PiB b-amyloid PET results with the centiloid scale. *J Nucl Med*. 2016;57:1233–7. <https://doi.org/10.2967/jnumed.115.171595>.
139. Cho SH, Choe YS, Kim HJ, et al. A new Centiloid method for 18F-florbetaben and 18F-flutemetamol PET without conversion to PiB. *Eur J Nucl Med Mol Imaging*. 2020;47:1938–48. <https://doi.org/10.1007/s00259-019-04596-x>.
140. Su Y, Flores S, Wang G, et al. Comparison of Pittsburgh compound B and florbetapir in cross-sectional and longitudinal studies. *Alzheimer's Dement Diagnosis, Assess Dis Monit*. 2019;11:180–90. <https://doi.org/10.1016/j.dadm.2018.12.008>.
141. Su Y, Flores S, Hornbeck RC, et al. Utilizing the Centiloid scale in cross-sectional and longitudinal PiB PET studies. *NeuroImage Clin*. 2018;19:406–16. <https://doi.org/10.1016/j.nicl.2018.04.022>.
142. Tudorascu DL, Minhas DS, Lao PJ, et al. The use of Centiloids for applying [11C]PiB classification cutoffs across region-of-interest delineation methods. *Alzheimer's Dement Diagnosis, Assess Dis Monit*. 2018;10:332–9. <https://doi.org/10.1016/j.dadm.2018.03.006>.
143. Navitsky M, Joshi AD, Kennedy I, et al. Standardization of amyloid quantitation with florbetapir standardized uptake value ratios to the Centiloid scale. *Alzheimers Dement*. 2018;14:1565–71. <https://doi.org/10.1016/j.jalz.2018.06.1353>.
144. Yun HJ, Moon SH, Kim HJ, et al. Centiloid method evaluation for amyloid PET of subcortical vascular dementia. *Sci Rep*. 2017;7. <https://doi.org/10.1038/s41598-017-16236-1>.
145. Buckley CJ, Foley C, Battle M, et al. AmyPype: an automated system to quantify AMYPAD's [18F]flutemetamol and [18F]florbetaben images including regional SUVR and Centiloid analysis. *Eur J Nucl Med Mol Imaging*. 2019;46:S323–4.
146. Royse SK, Minhas DS, Lopresti BJ, et al. Validation of amyloid PET positivity thresholds in centiloids: a multisite PET study approach. *Alzheimers Res Ther*. 2021;13:1–10. <https://doi.org/10.1186/s13195-021-00836-1>.
147. Salvadó G, Molinuevo JL, Brugulat-Serrat A, et al. Centiloid cut-off values for optimal agreement between PET and CSF core AD biomarkers. *Alzheimers Res Ther*. 2019;11:1–12. <https://doi.org/10.1186/s13195-019-0478-z>.
148. La Joie R, Ayakta N, Seeley WW, et al. Multisite study of the relationships between antemortem [11C]PiB-PET Centiloid values and postmortem measures of Alzheimer's disease neuropathology. *Alzheimers Dement*. 2019;15:205–16. <https://doi.org/10.1016/j.jalz.2018.09.001>.
149. Amadoru S, Doré V, McLean CA, et al. Comparison of amyloid PET measured in Centiloid units with neuropathological findings in Alzheimer's disease. *Alzheimers Res Ther*. 2020;12:1–8. <https://doi.org/10.1186/s13195-020-00587-5>.
150. Milà-Alomà M, Shekari M, Salvadó G, et al. Cognitively unimpaired individuals with a low burden of A β pathology have a distinct CSF biomarker profile. *Alzheimers Res Ther*. 2021;13:1–12. <https://doi.org/10.1186/s13195-021-00863-y>.
151. Jack CR, Wiste HJ, Weigand SD, et al. Age-specific and sex-specific prevalence of cerebral β -amyloidosis, tauopathy, and neurodegeneration in cognitively unimpaired individuals aged 50–95 years: a cross-sectional study. *Lancet Neurol*. 2017;16:435–44. [https://doi.org/10.1016/S1474-4422\(17\)30077-7](https://doi.org/10.1016/S1474-4422(17)30077-7).
152. Salvadó G, Milà-Alomà M, Shekari M, et al. Cerebral amyloid- β load is associated with neurodegeneration and gliosis: mediation by p-tau and interactions with risk factors early in the Alzheimer's continuum. *Alzheimers Dement*. 2021;17:788–800. <https://doi.org/10.1002/alz.12245>.
153. Farrell ME, Jiang S, Schultz AP, et al. Defining the lowest threshold for amyloid-PET to predict future cognitive decline and amyloid accumulation. *Neurology*. 2021;96:e619–31. <https://doi.org/10.1212/WNL.00000000000011214>.
154. Farrell ME, Chen X, Rundle MM, et al. Regional amyloid accumulation and cognitive decline in initially amyloid-negative adults. *Neurology*. 2018;91:E1809–21. <https://doi.org/10.1212/WNL.0000000000006469>.
155. van der Kall LM, Truong T, Burnham SC, et al. Association of β -amyloid level, clinical progression, and longitudinal cognitive change in normal older individuals. *Neurology*. 2021;96:e662–70. <https://doi.org/10.1212/WNL.00000000000011222>.
156. Hanseew BJ, Malotau V, Dricot L, et al. Defining a Centiloid scale threshold predicting long-term progression to dementia in patients attending the memory clinic: an [18F] flutemetamol amyloid PET study. *Eur J Nucl Med Mol Imaging*. 2021;48:302–10. <https://doi.org/10.1007/s00259-020-04942-4>.
157. Bischof GN, Jacobs HIL. Subthreshold amyloid and its biological and clinical meaning: long way ahead. *Neurology*. 2019;93:72–9. <https://doi.org/10.1212/WNL.0000000000007747>.
158. Aisen PS, Zhou J, Irizarry MC, et al. AHEAD 3-45 study design: a global study to evaluate the efficacy and safety of treatment with BAN2401 for 216 weeks in preclinical Alzheimer's disease with intermediate amyloid (A3 trial) and elevated amyloid (A45 trial). *Alzheimers Dement*. 2020;16:e044511. <https://doi.org/10.1002/alz.044511>.
159. Salloway S, Farlow M, McDade E, et al. A trial of gantenerumab or solanezumab in dominantly inherited Alzheimer's disease. *Nat Med*. 2021;27:1187–96. <https://doi.org/10.1038/s41591-021-01369-8>.
160. Bateman RJ, Aschenbrenner AJ, Benzinger TLS, et al. Overview of dominantly inherited AD and top-line DIAN-TU results of solanezumab and gantenerumab. *Alzheimers Dement*. 2020;16:e041129. <https://doi.org/10.1002/alz.041129>.
161. Lopes Alves I, Heeman F, Collij LE, et al. Strategies to reduce sample sizes in Alzheimer's disease primary and secondary prevention trials using longitudinal amyloid PET imaging. *Alzheimers Res Ther*. 2021;13. <https://doi.org/10.1186/s13195-021-00819-2>.
162. Knopman DS, Lundt ES, Therneau TM, et al. Association of initial β -amyloid levels with subsequent flortaucipir positron emission tomography changes in persons without cognitive impairment. *JAMA Neurol*. 2021;78:217–28. <https://doi.org/10.1001/jamaneurol.2020.3921>.
163. Petrover D, Giliberto L, Clouston S, et al. Semiquantitative approach to amyloid PET interpretation in clinical practice. *J Nucl Med*. 2021;62:1068 LP–1068.
164. Curry S, Patel N, Fakhry-Darian D, et al (2019) Advances in neurodegenerative and psychiatric imaging special feature: full paper: quantitative evaluation of beta-amyloid brain PET imaging in dementia: a comparison between two commercial software packages and the clinical report. *Br J Radiol* 92. <https://doi.org/10.1259/bjr.20181025>
165. Lilja J, Thurfjell L, Sörensen J. Visualization and quantification of 3-dimensional stereotactic surface projections for 18F-flutemetamol pet using variable depth. *J Nucl Med*. 2016;57:1078–83. <https://doi.org/10.2967/jnumed.115.169169>.
166. Cho H, Lee HS, Choi JY, et al. Predicted sequence of cortical tau and amyloid- β deposition in Alzheimer disease spectrum. *Neurobiol Aging*. 2018;68:76–84. <https://doi.org/10.1016/j.neurobiolaging.2018.04.007>.
167. Cho H, Choi JY, Hwang MS, et al. In vivo cortical spreading pattern of tau and amyloid in the Alzheimer disease spectrum. *Ann Neurol*. 2016;80:247–58. <https://doi.org/10.1002/ana.24711>.

168. Baek MS, Cho H, Lee HS, et al. Temporal trajectories of in vivo tau and amyloid- β accumulation in Alzheimer's disease. *Eur J Nucl Med Mol Imaging*. 2020;47:2879–86. <https://doi.org/10.1007/s00259-020-04773-3>.
169. Whittington A, Sharp DJ, Gunn RN. Spatiotemporal distribution of B-amyloid in Alzheimer disease is the result of heterogeneous regional carrying capacities. *J Nucl Med*. 2018;59:822–7. <https://doi.org/10.2967/jnumed.117.194720>.
170. Zammit MD, Laymon CM, Bethausser TJ, et al. Amyloid accumulation in Down syndrome measured with amyloid load. *Alzheimer's Dement Diagnosis, Assess Dis Monit*. 2020;12:e12020. <https://doi.org/10.1002/dad2.12020>.
171. Zammit MD, Tudorascu DL, Laymon CM, et al. PET measurement of longitudinal amyloid load identifies the earliest stages of amyloid-beta accumulation during Alzheimer's disease progression in Down syndrome. *Neuroimage*. 2021;228:117728. <https://doi.org/10.1016/j.neuroimage.2021.117728>.
172. Lilja J, Leuz A, Chiotis K, et al. Spatial normalization of 18 F-flutemetamol PET images using an adaptive principal-component template. *J Nucl Med*. 2019;60:285–91. <https://doi.org/10.2967/jnumed.118.207811>.
173. Haller S, Montandon ML, Lilja J, et al. PET amyloid in normal aging: direct comparison of visual and automatic processing methods. *Sci Rep*. 2020;10:1–8. <https://doi.org/10.1038/s41598-020-73673-1>.
174. Schreiber S, Landau SM, Fero A, et al. Comparison of visual and quantitative florbetapir F 18 positron emission tomography analysis in predicting mild cognitive impairment outcomes. *JAMA Neurol*. 2015;72:1183–90. <https://doi.org/10.1001/jamaneurol.2015.1633>.
175. Vandenberghe R, Van Laere K, Ivanoiu A, et al. 18F-flutemetamol amyloid imaging in Alzheimer disease and mild cognitive impairment a phase 2 trial. *Ann Neurol*. 2010;68:319–29. <https://doi.org/10.1002/ana.22068>.
176. Verfaillie SCJ, Golla SSV, Timmers T, et al. Repeatability of parametric methods for [18F]florbetapir imaging in Alzheimer's disease and healthy controls: a test-retest study. *J Cereb Blood Flow Metab*. 2021;41:569–78. <https://doi.org/10.1177/0271678X20915403>.
177. Mattsson N, Insel PS, Landau S, et al. Diagnostic accuracy of CSF Ab42 and florbetapir PET for Alzheimer's disease. *Ann Clin Transl Neurol*. 2014;1:534–43. <https://doi.org/10.1002/acn3.81>.
178. Doré V, Bullich S, Rowe CC, et al. Comparison of 18F-florbetaben quantification results using the standard Centiloid, MR-based, and MR-less CapAIBL® approaches: validation against histopathology. *Alzheimers Dement*. 2019;15:807–16. <https://doi.org/10.1016/j.jalz.2019.02.005>.
179. Patel N, Fakhry-Darian D, Nijran K, et al. Assessment and optimisation of hermes amyloid BRASS as a quantitative diagnostic tool in reporting 18F-florbetapir (Amyvid) investigations. *J Nucl Med*. 2018;59.
180. Leuz A, Heurling K, De Santi S, et al. Validation of a spatial normalization method using a principal component derived adaptive template for [18F]florbetaben PET. *Am J Nucl Med Mol Imaging*. 2020;10:161–7.
181. Choi WH, Um YH, Jung WS, Kim SH. Automated quantification of amyloid positron emission tomography: a comparison of PMOD and MIMneuro. *Ann Nucl Med*. 2016;30:682–9. <https://doi.org/10.1007/s12149-016-1115-6>.
182. Fleisher AS, Chen K, Liu X, et al. Using positron emission tomography and florbetapir F 18 to image cortical amyloid in patients with mild cognitive impairment or dementia due to Alzheimer disease. *Arch Neurol*. 2011;68:1404–11. <https://doi.org/10.1001/archneurol.2011.150>.
183. Bourgeat P, Dore V, Fripp J, et al. Computational analysis of PET by AIBL (CapAIBL): a cloud-based processing pipeline for the quantification of PET images. *Med Imaging 2015 Image Process*. 2015;9413:94132V. <https://doi.org/10.1117/12.2082492>.
184. Chincarini A, Sensi F, Rei L, et al. Standardized uptake value ratio-independent evaluation of brain amyloidosis. *J Alzheimers Dis*. 2016;54:1437–57. <https://doi.org/10.3233/JAD-160232>.
185. Bullich S, Seibyl J, Catafau AM, et al. Optimized classification of 18F-florbetaben PET scans as positive and negative using an SUVR quantitative approach and comparison to visual assessment. *NeuroImage Clin*. 2017;15:325–32. <https://doi.org/10.1016/j.nicl.2017.04.025>.
186. Ataka S, Takeda A, Mino T, et al. Ic-P-034: comparison of [18F] flutemetamol and [11C] PIB PET images. *Alzheimers Dement*. 2014;10:P21–1. <https://doi.org/10.1016/j.jalz.2014.05.038>.
187. Villemagne VL, Mulligan RS, Pejoska S, et al. Comparison of 11C-PiB and 18F-florbetaben for A β imaging in ageing and Alzheimer's disease. *Eur J Nucl Med Mol Imaging*. 2012;39:983–9. <https://doi.org/10.1007/s00259-012-2088-x>.
188. Chincarini A, Peira E, Morbelli S, et al. Semi-quantification and grading of amyloid PET: a project of the European Alzheimer's Disease Consortium (EADC). *NeuroImage Clin*. 2019;23:101846. <https://doi.org/10.1016/j.nicl.2019.101846>.
189. Ceccaldi M, Jonveaux T, Verger A, et al. Added value of 18F-florbetaben amyloid PET in the diagnostic workup of most complex patients with dementia in France: a naturalistic study. *Alzheimers Dement*. 2018;14:293–305. <https://doi.org/10.1016/j.jalz.2017.09.009>.
190. Harn NR, Hunt SL, Hill J, et al. Augmenting amyloid PET interpretations with quantitative information improves consistency of early amyloid detection. *Clin Nucl Med*. 2017;42:577–81. <https://doi.org/10.1097/RLU.0000000000001693>.
191. Schwarz AJ. The use, standardization, and interpretation of brain imaging data in clinical trials of neurodegenerative disorders. *Neurotherapeutics*. 2021;18:686–708. <https://doi.org/10.1007/s13311-021-01027-4>.
192. Jansen WJ, Janssen O, Tijms BM, et al. Prevalence estimates of amyloid abnormality across the Alzheimer disease clinical spectrum. *JAMA Neurol*. 2022. <https://doi.org/10.1001/jamaneurol.2021.5216>.
193. Cummings J, Salloway S. Aducanumab: appropriate use recommendations. *Alzheimers Dement*. 2021. <https://doi.org/10.1002/alz.12444>.
194. Shekari M, Salvadó G, Battle MR, et al. Evaluating robustness of the Centiloid scale against variations in amyloid PET image resolution. *Alzheimers Dement*. 2021;17. <https://doi.org/10.1002/alz.055726>.
195. Heeman F, Yaqub M, Hendriks J, et al. Parametric imaging of dual-time window [18F]flutemetamol and [18F]florbetaben studies. *Neuroimage*. 2021;234. <https://doi.org/10.1016/j.neuroimage.2021.117953>.
196. Cummings J, Aisen P, Lemere C, et al. Aducanumab produced a clinically meaningful benefit in association with amyloid lowering. *Alzheimers Res Ther*. 2021;13:1–3. <https://doi.org/10.1186/s13195-021-00838-z>.
197. Sevigny J, Chiao P, Bussière T, et al. The antibody aducanumab reduces A β plaques in Alzheimer's disease. *Nature*. 2016;537:50–6. <https://doi.org/10.1038/nature19323>.
198. Haeblerlein SB, von Hehn C, Tian Y, et al. Emerge and engage topline results: phase 3 studies of aducanumab in early Alzheimer's disease. *Alzheimers Dement*. 2020;16:1–60. <https://doi.org/10.1002/alz.047259>.
199. Grothe MJ, Barthel H, Sepulcre J, et al. In vivo staging of regional amyloid deposition. *Neurology*. 2017;89:2031–8. <https://doi.org/10.1212/WNL.0000000000004643>.
200. McMillan CT, Chételat G. Amyloid “accumulators”: the next generation of candidates for amyloid-targeted clinical trials?

- Neurology. 2018;90:759–60. <https://doi.org/10.1212/WNL.0000000000005362>.
201. Ben BF, Mariano-Goulart D, Payoux P. Comparison of CSF markers and semi-quantitative amyloid PET in Alzheimer's disease diagnosis and in cognitive impairment prognosis using the ADNI-2 database. *Alzheimers Res Ther*. 2017;9:1–13. <https://doi.org/10.1186/s13195-017-0260-z>.
 202. Palmqvist S, Schöll M, Strandberg O, et al. Earliest accumulation of β -amyloid occurs within the default-mode network and concurrently affects brain connectivity. *Nat Commun*. 2017;8:1–13. <https://doi.org/10.1038/s41467-017-01150-x>.
 203. Thal DR, Rüb U, Orantes M, Braak H. Phases of A β -deposition in the human brain and its relevance for the development of AD. *Neurology*. 2002;58:1791–800. <https://doi.org/10.1212/WNL.58.12.1791>.
 204. Collij LE, Konijnenberg E, Reimand J, et al. Assessing amyloid pathology in cognitively normal subjects using 18F-flutemetamol PET: comparing visual reads and quantitative methods. *J Nucl Med*. 2019;60:541–7. <https://doi.org/10.2967/jnumed.118.211532>.
 205. Cohen AD, Mowrey W, Weissfeld LA, et al. Classification of amyloid-positivity in controls: comparison of visual read and quantitative approaches. *Neuroimage*. 2013;71:207–15. <https://doi.org/10.1016/j.neuroimage.2013.01.015>.
 206. Chételat G, Murray ME. Amyloid PET scan: staging beyond reading? *Neurology*. 2017;89:2029–30. <https://doi.org/10.1212/WNL.0000000000004678>.
 207. Mattsson N, Palmqvist S, Stomrud E, et al. Staging β -amyloid pathology with amyloid positron emission tomography. *JAMA Neurol*. 2019;76:1319–29. <https://doi.org/10.1001/jamaneurol.2019.2214>.
 208. Collij LE, Heeman F, Salvadó G, et al. Multitracer model for staging cortical amyloid deposition using PET imaging. *Neurology*. 2020;95:e1538–53. <https://doi.org/10.1212/WNL.0000000000010256>.
 209. O'bryant SE, Johnson LA, Barber RC, et al (2021) The Health & Aging Brain among Latino Elders (HABLE) study methods and participant characteristics. *Alzheimer's Dement Diagnosis, Assess Dis Monit* 13:. <https://doi.org/10.1002/dad2.12202>
 210. Windon C, Dilworth-Anderson P, Carrillo MC, et al. IDEAS and new IDEAS: amyloid PET in diverse populations. *Alzheimers Dement*. 2021;17:e051946. <https://doi.org/10.1002/ALZ.051946>.
 211. Iaccarino L, La Joie R, Koeppe R, et al. rPOP: robust PET-only processing of community acquired heterogeneous amyloid-PET data. *Neuroimage*. 2022;246:118775. <https://doi.org/10.1016/j.neuroimage.2021.118775>.
 212. Kim S, Lee P, Oh KT, et al. Deep learning-based amyloid PET positivity classification model in the Alzheimer's disease continuum by using 2-[18F]FDG PET. *EJNMMI Res*. 2021;11:1–14. <https://doi.org/10.1186/s13550-021-00798-3>.
 213. Shirbandi K, Khalafi M, Mirza-Aghazadeh-Attari M, et al. Accuracy of deep learning model-assisted amyloid positron emission tomography scan in predicting Alzheimer's disease: a systematic review and meta-analysis. *Informatics Med Unlocked*. 2021;25:100710. <https://doi.org/10.1016/j.imu.2021.100710>.
 214. Kim JY, Suh HY, Ryoo HG, et al. Amyloid PET quantification via end-to-end training of a deep learning. *Nucl Med Mol Imaging*. 2019;53(2010):340–8. <https://doi.org/10.1007/s13139-019-00610-0>.
 215. Doré V, Krishnadas N, Bourgeat P, et al. Relationship between amyloid and tau levels and its impact on tau spreading. *Eur J Nucl Med Mol Imaging*. 2021;48:2225–32. <https://doi.org/10.1007/s00259-021-05191-9>.
 216. Ossenkoppele R, Smith R, Mattsson-Carlgrén N, et al. Accuracy of tau positron emission tomography as a prognostic marker in preclinical and prodromal Alzheimer disease: a head-to-head comparison against amyloid positron emission tomography and magnetic resonance imaging. *JAMA Neurol*. 2021;78:961–71. <https://doi.org/10.1001/jamaneurol.2021.1858>.
 217. Yamao T, Miwa K, Wagatsuma K, et al. Centiloid scale analysis for 18F-THK5351 PET imaging in Alzheimer's disease. *Phys Medica*. 2021;82:249–54. <https://doi.org/10.1016/j.ejmp.2021.02.017>.

Publisher's note Springer Nature remains neutral with regard to jurisdictional claims in published maps and institutional affiliations.

Authors and Affiliations

Hugh G. Pemberton^{1,2,3}  · Lyduine E. Collij⁴ · Fiona Heeman⁴  · Ariane Bollack² · Mahnaz Shekari^{5,6,7} · Gemma Salvadó^{5,8}  · Isadora Lopes Alves^{4,9} · David Vallez Garcia⁴  · Mark Battle^{1,8}  · Christopher Buckley¹ · Andrew W. Stephens¹⁰  · Santiago Bullich¹⁰  · Valentina Garibotto^{11,12} · Frederik Barkhof^{2,3,4}  · Juan Domingo Gispert^{5,6,7,13} · Gill Farrar¹ · on behalf of the AMYPAD consortium

¹ GE Healthcare, Amersham, UK

² Centre for Medical Image Computing (CMIC), Department of Medical Physics and Bioengineering, University College London, London, UK

³ UCL Queen Square Institute of Neurology, University College London, London, UK

⁴ Department of Radiology and Nuclear Medicine, Amsterdam Neuroscience, Amsterdam UMC, Vrije Universiteit Amsterdam, Amsterdam, The Netherlands

⁵ Barcelonaβeta Brain Research Center (BBRC), Pasqual Maragall Foundation, Barcelona, Spain

⁶ Universitat Pompeu Fabra, Barcelona, Spain

⁷ IMIM (Hospital del Mar Medical Research Institute), Barcelona, Spain

⁸ Clinical Memory Research Unit, Department of Clinical Sciences, Lund University, Malmö, Sweden

⁹ Brain Research Center, Amsterdam, The Netherlands

¹⁰ Life Molecular Imaging GmbH, Berlin, Germany

¹¹ Division of Nuclear Medicine and Molecular Imaging, University Hospitals of Geneva, Geneva, Switzerland

¹² NIMTLab, Faculty of Medicine, University of Geneva, Geneva, Switzerland

¹³ Centro de Investigación Biomédica en Red Bioingeniería, Biomateriales y Nanomedicina, Madrid, Spain